

**INVESTIGATION OF THE
ATMOSPHERIC OZONE FORMATION
POTENTIAL OF SELECTED CARBONATES**

Report to
ExxonMobil Chemical Company

by

William P. L. Carter, Dongmin Luo, and Irina L. Malkina

November 17, 2000

College of Engineering
Center for Environmental Research and Technology
University of California
Riverside, California 92521

ABSTRACT

A series of environmental chamber experiments and computer model calculations were carried out to assess the atmospheric ozone formation potentials of dimethyl carbonate and methyl isopropyl carbonate. The experiments consisted of determining the effects of these compounds on NO oxidation, ozone formation, OH radical levels, and other measures of reactivity when added to three types of simulated model photochemical smog systems. Both compounds were found to enhance NO oxidation and O₃ formation rates under all conditions, though relatively large amounts of dimethyl carbonate had to be added to have measurable effects. The addition of methyl isopropyl carbonate caused increased formation of formaldehyde and acetone, while dimethyl carbonate had no effects on formaldehyde or other organic products that could be monitored. The rate constant for the reaction of OH radicals with dimethyl carbonate was measured to be $2.55 \pm 0.64 \times 10^{-12} \text{ cm}^3 \text{ molec}^{-1} \text{ s}^{-1}$, using a relative rate method with propane as the reference compound. Atmospheric reaction mechanisms for these compounds were developed using the measured OH radical rate constants and estimates for the subsequent reactions. These mechanisms were found to give good predictions of the effects of these compounds on O₃ formation, NO oxidation, and product formation observed in the chamber experiments. These mechanisms were then incorporated in the overall SAPRC-99 mechanism and used to predict the atmospheric ozone impacts of these compounds under various atmospheric conditions. The ozone impacts of dimethyl carbonate were found to be no more than ~30% that of ethane on a mass basis, suggesting that it may be appropriate to exempt this compound from regulation as a VOC ozone precursor under the current standards used by the EPA. The ozone impacts of methyl isopropyl carbonate were found to be about twice those of ethane on a mass basis, comparable to that of propane, and about 1/5 to 1/3 that of the mixture used to represent reactive VOC emissions from all sources.

ACKNOWLEDGEMENTS

The authors acknowledge Mr. Dennis Fitz for assistance in administering this program, Mr. Kurt Bumiller with assistance in carrying out the environmental chamber experiments, and Dr. Roger Atkinson for helpful discussions.

This work was funded by ExxonMobil Chemical Company. The opinions and conclusions expressed in this report are entirely those of the primary author, Dr. William P. L. Carter. Mention of trade names or commercial products do not constitute endorsement or recommendation for use.

TABLE OF CONTENTS

INTRODUCTION.....	1
EXPERIMENTAL AND DATA ANALYSIS METHODS.....	3
Environmental Chamber Experiments.....	3
Overall Experimental Approach.....	3
Environmental Chamber	4
Experimental Procedures.....	5
Kinetic Experiments	5
Analytical Methods.....	7
Characterization Methods	8
Temperature	8
Blacklight Light Source	8
Dilution	8
Reactivity Data Analysis Methods	9
CHEMICAL MECHANISMS AND MODELING METHODS	11
Chemical Mechanism	11
General Atmospheric Photooxidation Mechanism.....	11
Atmospheric Reactions of Dimethyl Carbonate.....	11
Atmospheric Reactions of Methyl Isopropyl Carbonate	13
Modeling Methods.....	16
Environmental Chamber Simulations	16
Atmospheric Reactivity Simulations.....	17
EXPERIMENTAL AND MECHANISM EVALUATION RESULTS	18
Relative Rate Constant Measurements	18
Summary of Environmental Chamber Experiments and Characterization Results	23
Dimethyl Carbonate Reactivity Experiments	29
Methyl Isopropyl Carbonate Reactivity Experiments.....	31
ATMOSPHERIC REACTIVITY CALCULATIONS	33
Scenarios Used for Reactivity Assessment.....	33
Base Case Scenarios.....	34
Adjusted NO _x scenarios	36
NO _x Conditions in the Base Case Scenarios	36
Quantification of Atmospheric Reactivity	36
Results.....	38
CONCLUSIONS.....	42
REFERENCES.....	43
APPENDIX A. MECHANISM LISTING AND TABULATIONS	47

LIST OF TABLES

Table 1.	Detailed mechanism for the reactions of OH radicals with methyl isopropyl carbonate as generated using the SAPRC-99 mechanism generation system, with corrected estimates for ester rearrangement reactions.....	15
Table 2.	Summary of conditions and measurement data for the kinetic experiments carried out for this program.	20
Table 3.	Summary of Results of OH Radical Rate Constant Measurements.....	23
Table 4.	Chronological listing of the environmental chamber experiments carried out for this program.	24
Table 5.	Summary of conditions and selected results of the environmental chamber reactivity experiments with dimethyl carbonate and methyl isopropyl carbonate.....	29
Table 6.	Summary of the conditions of the scenarios used for atmospheric reactivity assessment.....	35
Table 7.	Atmospheric incremental reactivities calculated for the base ROG mixture, ethane, dimethyl carbonate (DMC), methyl isopropyl carbonate (MIPR-CB) and propane.....	39
Table 8.	Atmospheric relative reactivities calculated for ethane, dimethyl carbonate (DMC), methyl isopropyl carbonate (MIPR-CB) and propane.	40
Table A-1.	Listing of the model species in the mechanism used in the model simulations discussed in this report.....	48
Table A-2.	Listing of the reactions in the mechanism used in the model simulations discussed in this report. See Carter (2000) for documentation.	51
Table A-3.	Listing of the absorption cross sections and quantum yields for the photolysis reactions.....	60
Table A-4.	Chamber wall effect and background characterization parameters used in the environmental chamber model simulations for mechanism evaluation.....	69

LIST OF FIGURES

Figure 1.	Plots of Equation (IV) for n-butane, benzene, and methyl isopropyl carbonate, with propane as the test compound.	22
Figure 2.	Selected results of the low NO _x mini-surrogate side equivalency test experiment, and comparison with comparable data obtained in the low NO _x mini-surrogate experiments with added dimethyl carbonate.	28
Figure 3.	Selected experimental and calculated results of the incremental reactivity experiments with Dimethyl Carbonate	30
Figure 4.	Selected experimental and calculated results of the incremental reactivity experiments with Methyl Isopropyl Carbonate.	32

INTRODUCTION

Ozone in photochemical smog is formed from the gas-phase reactions of volatile organic compounds (VOCs) and oxides of nitrogen (NO_x) in sunlight. Although Houston and Los Angeles currently have the worst ozone problems in the United States, other areas of the country also have episodes where ozone exceeds the federal air quality standard. Ozone control strategies in the past have focused primarily on VOC controls, though the importance of NO_x control has become recognized in recent years. VOC and NO_x controls have differing effects on ozone formation. NO_x is required for ozone formation, and if the levels of NO_x are low compared to the levels of reactive VOCs, then changing VOC emissions will have relatively little effect on ozone. Since NO_x is removed from the atmosphere more rapidly than VOCs, ozone in areas far downwind from the primary sources tend to be more NO_x limited, and thus less responsive to VOC controls. VOC controls tend to reduce the rate that O_3 is formed when NO_x is present, so VOC controls are the most beneficial in reducing O_3 in the urban source areas, where NO_x is relatively plentiful, and where O_3 yields are determined primarily by how rapidly it is being formed. Because of this, any comprehensive ozone control strategy should involve reduction of emissions of both NO_x and VOCs.

Many different types of VOCs are emitted into the atmosphere, each reacting at different rates and having different mechanisms for their reactions. Because of this, they can differ significantly in their effects on ozone formation, or their “reactivity”. Some compounds, such as CFCs, do not react in the lower atmosphere at all, and thus make no contribution to ground-level ozone formation. Others, such as methane, react and contribute to ozone formation, but react so slowly that their practical effect on ozone formation in urban atmospheres is negligible. Obviously, it does not make sense to regulate such compounds as ozone precursors. In recognition of this, the EPA has exempted certain compounds from such regulations on the basis of having “negligible” effects on ozone formation. Although the EPA has no formal policy on what constitutes “negligible” reactivity, in practice it has used the ozone formation potential of ethane as the standard in this regard. Therefore, the ozone formation potential of a compound relative to ethane is of particular interest when assessing whether it might be a likely candidate for exemption from regulation as an ozone precursor.

Many VOCs that would not be judged to have “negligible” reactivity under the current criterion might still have much lower ozone formation potential than average, and substituting emissions of highly reactive VOCs with such moderate-to-low reactivity VOCs would be expected to result in air quality improvements. Although the current EPA policies do not encourage such substitutions, it has been proposed to implement reactivity-based policies on a voluntary basis in consumer product regulations in California (CARB, 1999), and the EPA is currently re-evaluating its reactivity-based VOC policies (Dimitriades, 1999, RRWG, 1999). Mc.Bride et al (1997) showed that adopting reactivity-based VOC control policies could result in significant cost savings in ozone reduction strategies, though a number of difficult policy and enforcement issues need to be resolved (RRWG, 1999). Although regulatory

approaches that appropriately deal with differences in VOC reactivity are still evolving, it is clear that producers of solvent VOCs will need to know how their VOCs might be classified under any such system, so they can appropriately adapt to reactivity-based policies once they are implemented. This requires an ability to reliably estimate the ozone impacts of the VOCs of interest.

Dimethyl carbonate, $\text{CH}_2\text{OC}(\text{O})\text{OCH}_3$, and methyl isopropyl carbonate, $\text{CH}_3\text{OC}(\text{O})\text{OCH}(\text{CH}_3)_2$ are compounds that have potential markets for various commercial applications. If these compounds were shown to have sufficiently low ozone reactivity that they could be exempted from regulation as an ozone precursor, their potential marketability would be enhanced. Exxon Chemical Company (now ExxonMobil) contracted the College of Engineering Center for Environmental Research and Technology (CE-CERT) to carry out the experimental and modeling study needed to provide data to assess this. This involves conducting environmental chamber experiments to determine the effects of these compounds on O_3 formation and other measures of air quality under various conditions, and then using the results to determine if current estimated mechanisms for them can appropriately predict their atmospheric impacts. Once their predictive capabilities are established, the mechanisms can then be used in model calculations to determine their ozone impacts under various atmospheric conditions. The results can then be compared for the ozone impacts calculated for ethane under those same conditions, to determine if they have sufficiently low ozone impact under the standards currently used by the EPA to be exempted from regulation as an ozone precursor. The results of this study are documented in this report.

EXPERIMENTAL AND DATA ANALYSIS METHODS

Environmental Chamber Experiments

Overall Experimental Approach

Most of the experiments for this program consisted of environmental chamber experiments to make measurements of “incremental reactivities” of the subject compounds under various conditions. These involve two types of irradiations of model photochemical smog mixtures. The first is a “base case” experiment where a mixture of reactive organic gases (ROGs) representing those present in polluted atmospheres (the “ROG surrogate”) is irradiated in the presence of oxides of nitrogen (NO_x) in air. The second is the “test” experiment that consists of repeating the base case irradiation except that the VOC whose reactivity is being assessed is also added. The differences between the results of these experiments provide a measure of the atmospheric impact of the test compound, and the difference relative to the amount added is a measure of its reactivity. To provide data concerning the reactivities of a test compound under varying atmospheric conditions, three types of base case experiments were carried out:

Mini-Surrogate Experiments. This base case employs a simplified ROG surrogate and relatively low ROG/NO_x ratios. Low ROG/NO_x ratios represent “maximum incremental reactivity” (MIR) conditions, which are most sensitive to VOC effects. This is useful because it provides a sensitive test for the model, and also because it is most important that the model correctly predict a VOC's reactivity under conditions where the atmosphere is most sensitive to the VOCs. The ROG mini-surrogate mixture employed consisted of ethene, n-hexane, and m-xylene. It consists of the following average initial concentrations (in ppm): NO : 0.30, NO_2 : 0.10, n-hexane: 0.50, ethene: 0.85, and m-xylene: 0.14. This surrogate was employed in our previous studies (Carter et al, 1993; 1995a-c, 1997, 2000a), and was found to provide a more sensitive test of the mechanism than the more complex surrogates that more closely represent atmospheric conditions (Carter et al, 1995b). This high sensitivity to mechanistic differences makes the mini-surrogate experiments most useful for mechanism evaluation.

Full Surrogate Experiments. This base case employed a more complex ROG surrogate under somewhat higher, though still relatively low, ROG/NO_x conditions. While less sensitive to the mechanism employed, experiments with a more representative ROG surrogate are needed to evaluate the mechanism under conditions that more closely resembling the atmosphere. The ROG surrogate employed was the same as the 8-component “lumped molecule” surrogate as employed in our previous study (Carter et al. 1995b). Calculations have indicated that use of this 8-component mixture will give essentially the same results in incremental reactivity experiments as actual ambient mixtures (Carter et al. 1995b). It consists of the following average initial concentrations, in ppm: NO : 0.25, NO_2 : 0.05, n-butane: 0.40, n-octane: 0.10, ethene: 0.07, propene, 0.06, trans-2-butene: 0.06, toluene: 0.09, m-xylene 0.09, and formaldehyde: 0.10.

Full Surrogate, low NO_x Experiments. This base case employing the same 8-component “lumped molecule” surrogate as the full surrogate experiments described above, except that lower NO_x levels (higher ROG/NO_x ratios) were employed to represent NO_x-limited conditions. Such experiments are necessary to assess the ability of the model to properly simulate reactivities under conditions where NO_x is low. The initial ROG and NO_x reactant concentrations were comparable to those employed in our previous studies (Carter et al. 1995b, 1997, 2000a). The initial concentrations are the same as above except for 0.06 ppm of NO and 0.03 ppm of NO₂.

An appropriate set of control and characterization experiments necessary for assuring data quality and characterizing the conditions of the runs for mechanism evaluation were also carried out. These are discussed where relevant in the results or modeling methods sections (see also Carter et al, 1995c, 2000a).

Environmental Chamber

All experiments for this program were carried out using the CE-CERT “Dividable Teflon Chamber” (DTC) with a blacklight light source. This consists of two ~6000-liter 2-mil heat-sealed FEP Teflon reaction bags located adjacent to each other and fitted inside an 8' x 8' x 8' framework, and which uses two diametrically opposed banks of 32 Sylvania 40-W BL black lights as the light source. The lighting system in the DTC was found to provide so much intensity that only half the lights were used for irradiation. The air conditioner for the chamber room was turned on before and during the experiments. Four air blowers that are located in the bottom of the chamber were used to help cool the chamber as well as mix the contents of the chamber. The CE-CERT DTC is very similar to the SAPRC DTC which is described in detail elsewhere (Carter et al, 1995b,c).

The blacklight light source has the advantage of being relatively inexpensive to operate and provides a reasonably good simulation of natural sunlight in the region of the spectrum that is important in affecting most photolysis reactions of importance for non-aromatic VOCs (Carter et al, 1995c,d). This is therefore appropriate for studies of reactivities of compounds, such as these carbonates, which are not photoreactive or believed to form significant yields of photoreactive products whose action spectra are not well characterized.

The DTC is designed to allow simultaneous irradiations of experiments with and without added test reactants under the same reaction conditions. Since the chambers are actually two adjacent FEP Teflon reaction bags, two mixtures can be simultaneously irradiated using the same light source and with the same temperature control system. These two reaction bags are referred to as the two “sides” of the chambers (Side A and Side B) in the subsequent discussion. The sides are interconnected with two ports, each with a box fan, which rapidly exchange their contents to assure that base case reactants have equal concentrations in both sides. In addition, a fan is located in each of the reaction bags to rapidly mix the reactants within each chamber. The ports connecting the two reactors can then be closed to allow separate injections on each side, and separate monitoring of each side.

Experimental Procedures

The reaction bags were flushed with dry air produced by an AADCO air purification system for 14 hours (6pm-8am) on the nights before experiments. The continuous monitors were connected prior to reactant injection and the data system began logging data from the continuous monitoring systems. The reactants were injected as described below (see also Carter et al, 1993, 1995c). The common reactants were injected in both sides simultaneously using a three-way (one inlet and two outlets connected to side A and B respectively) bulb of 2 liters in the injection line and were well mixed before the chamber was divided. The contents of each side were blown into the other using two box fans located between them. Fans were used to mix the reactants in the chamber during the injection period, but these were turned off prior to the irradiation. The sides were then separated by closing the ports that connected them, after turning all the fans off to allow their pressures to equalize. After that, reactants for specific sides (the test compound in the case of reactivity experiments) were injected and mixed. After the run, the contents of the chamber were emptied by allowing the bags to collapse, and then the chamber was flushed with purified air. The contents of the reactors were vented into a fume hood.

The procedures for injecting the various types of reactants were as follows. The NO and NO₂ were prepared for injection using a high vacuum rack. Known pressures of NO, measured with MKS Baratron capacitance manometers, were expanded into Pyrex bulbs with known volumes, which were then filled with nitrogen (for NO) or oxygen (for NO₂). The contents of the bulbs were then flushed into the chamber with nitrogen. The gaseous reactants were prepared for injection either using a high vacuum rack or a gas-tight syringes whose amounts were calculated to achieve the desired concentrations in the chamber. Sufficiently volatile liquid reactants (which included both carbonates and the liquid surrogate components used in this study) were injected using a micro syringe into a 1-liter Pyrex bulb equipped with stopcocks on each end and a port for the injection of the liquid. Then one end of the bulb was attached to the injection port of the chamber and the other to a nitrogen source. The stopcocks were then opened, and the contents of the bulb were flushed into the chamber with a combination of nitrogen and heat gun for approximately 5 minutes. Formaldehyde was prepared in a vacuum rack system by heating paraformaldehyde in an evacuated bulb until the pressure corresponded to the desired amount of formaldehyde. The bulb was then closed and detached from the vacuum system and its contents were flushed into the chamber with dry air through the injection port. For DTC767 and following runs the common gaseous and liquid reactants were injected in both sides simultaneously using a “Y” shaped Pyrex tube.

Kinetic Experiments

In addition to the environmental chamber experiments for mechanism evaluation, a limited number of experiments were carried out to determine the rate constant for the reactions of OH radicals with methyl isopropyl carbonate, using a relative rate technique. Experiments were carried out using three different reactors and two different methods to generate OH radicals, as described below.

The reactors employed consisted either one side of the DTC chamber or a ~200-liter “pillow bag” constructed of 2 mil FEP Teflon film and placed inside an enclosure to permit blacklight irradiation. The light intensity for the pillow bag was approximately twice that used in the DTC. Pure dry air from an AADCO air purification system was used for all experiments, and all experiments were carried out at ambient temperature (approximately 295-298°K).

OH Radicals were generated either by the photolysis of nitrous acid (HONO) or by the photolysis of methyl nitrite in the presence of NO. The nitrous acid was prepared using the method of Febo et al (1995), which involves continuously passing low concentrations of gaseous HCl in humidified air through a stirred reactor containing sodium nitrite salt. This produced HONO in ppm quantities with no more than ~2% NO impurity, with no measurable HCl impurities as determined by bubbling the output of the HONO generator through water and analyzing the water for Cl⁻ ions. The output of this HONO generator was flushed into the reactor until the desired initial concentration was achieved, as determined by the flow rates, the HONO concentration output by the generator, and the volume of the reactor.

The methyl nitrate was synthesized at Roger Atkinson’s laboratory at the Air Pollution Research Center as described previously (Atkinson et al, 1981), and was transferred to our laboratory in the gas phase using ~0.6 liter Pyrex bulb covered with the black tape. The methyl nitrite was prepared for injection using a high vacuum rack as described above. The contents of the bulb were then flushed into the chamber with the Aadco air after all the reactants were already injected.

The general procedures for the experiments were similar regardless of the reactor or OH radical source employed. Approximately 0.1 - 0.3 ppb each of the compounds whose relative rates were to be determined were injected into the reactor along with the HONO or methyl nitrite/NO mixture. After the reactants were injected and mixed, the concentrations of the VOC reactants were monitored by gas chromatography until reproducible concentrations were measured. The analysis methods employed were the same as employed in the reactivity experiments, as described below. Then the lights were turned on for brief periods (initially 2.0 - 2.5 minutes, then longer as the experiment progressed) and then turned off. The reactant concentrations were measured between each irradiation. This continued until subsequent irradiations resulted in no change in reactant VOC concentrations. Typically, ~20 minutes of irradiations were carried out during a kinetic experiment.

The experiments employed propane as the reference compound, methyl isopropyl carbonate as the compound whose OH rate constant was to be determined and n-butane (in most cases) and benzene for verification purposes. Methyl pivalate was also present as a reactant in these experiments in approximately the same concentration range as used for the other compounds, but the data obtained were too scattered to be useful for kinetic purposes, and a discussion of this compound is beyond the scope of this report.

Analytical Methods

Ozone and nitrogen oxides (NO_x) were continuously monitored using commercially available continuous analyzers with Teflon sample lines inserted directly into the chambers. The sampling lines from each side of the chamber were connected to solenoids that switched from side to side every 10 minutes, so the instruments alternately collected data from each side. Ozone was monitored using a Dasibi 1003-AH UV photometric ozone analyzer and NO and total oxides of nitrogen (including organic nitrates and perhaps HNO_3) were monitored using a Teco Model 42 chemiluminescent NO/ NO_x monitor. The output of these instruments, along with that from the temperature sensors and the formaldehyde instrument, were attached to a computer data acquisition system, which recorded the data at 10 minutes intervals for ozone, NO_x and temperature (and at 15 minutes for formaldehyde), using 30 second averaging times. This yielded a sampling interval of 20 minutes for taking data from each side.

The Teco instrument and Dasibi CO analyzer were calibrated prior to each experiment using a certified NO and CO source and CSI gas-phase dilution system. The Dasibi ozone analyzer was calibrated against transfer standard ozone analyzer using transfer standard method in an interval of three months and was checked with CSI ozone generator for each experiment to assure that the instrument worked properly. The details were discussed elsewhere (Carter et al, 1995c)

Organic reactants other than formaldehyde were measured by gas chromatography with FID detection as described elsewhere (Carter et al. 1993; 1995c). GC samples were taken for analysis at intervals of about 20 minutes using 100 ml gas-tight glass syringes. These samples were taken from ports directly connected to the chamber after injection and before irradiation and at regular intervals after irradiation was started. The sampling method employed for injecting the sample onto the GC column depended on the volatility or “stickiness” of the compound. For analysis of the more volatile species, which includes both carbonates and all the other organic compounds monitored in this study, the contents of the syringe were flushed through a 10 ml and 5 ml stainless steel or 1/8' Teflon tube loop and subsequently injected onto the column by turning a gas sample valve.

The calibrations for the GC analyses for most compounds were carried out by sampling from chambers or vessels of known volume into which known amounts of the reactants were injected, as described previously (Carter et al, 1995c).

Formaldehyde was monitored using an adaptation of the diffusion scrubber method developed by Dasgupta et al (1988, 1990), as described by Carter et al (1995c). It was calibrated using a formaldehyde diffusion tube whose weight loss was monitored over time. The system cycled between zero, calibrate, and sample modes to correct for zero and span drifts.

Characterization Methods

Temperature

Three temperature thermocouples were used to monitor the chamber temperature, two of which were located in the sampling line of continuous analyzers to monitor the temperature in each side. The third one was located in the outlet of the air conditioning system used to control the chamber temperature. The temperature range in these experiments was typically 25-30 C.

Blacklight Light Source

The light intensity in the DTC chamber was monitored by periodic NO₂ actinometry experiments utilizing the quartz tube method of Zafonte et al (1977), with the data analysis method modified as discussed by Carter et al. (1995c). The results of these experiments were tracked over time, and there was a gradual decrease in light intensity over time during most of the operational lifetime of this chamber. The actinometry results around the time of these experiments were fit reasonably well by a straight line up to run DTC704, and this was used to determine the NO₂ photolysis rates used for modeling those runs. This yielded assigned NO₂ photolysis rates of 0.164 min⁻¹ for DTC692, the first DTC run for this project, and 0.161 min⁻¹ for run DTC704. For runs after DTC704 the results of the actinometry experiments did not indicate a significant decline in light intensity and NO₂ photolysis rate used for modeling was the average of the experimental measurements for this period, which was 0.161 min⁻¹.

The spectrum of the blacklight light source was periodically measured using a LiCor LI-1800 spectroradiometer, and was found to be essentially the same as the general blacklight spectrum recommended by Carter et al (1995c) for use in modeling blacklight chamber experiments

Dilution

The dilution of the chambers due to sampling is expected to be small because the flexible reaction bags can collapse as samples are withdrawn for analysis. Also, the chambers were designed to operate under slightly positive pressure, so any small leaks would result in reducing the bag volume rather than diluting the contents of the chamber. Information concerning dilution in an experiment can be obtained from relative rates of decay of added VOCs that react with OH radicals with differing rate constants (Carter et al. 1993; 1995c). Most experiments had a more reactive compound such as m-xylene and n-octane present either as a reactant or added in trace amounts to monitor OH radical levels. Trace amounts (~0.1 ppm) of n-butane were also added to experiments if needed to provide a less reactive compound for monitoring dilution. In addition, specific dilution check experiments such as CO dark decay measurements were periodically carried out. Based on these results, the dilution rate was found to be negligible in this chamber during this period, being less than 0.3% per hour in all runs, and usually less than 0.1% per hour.

Reactivity Data Analysis Methods

As indicated above, most of the experiments for this program consisted of simultaneous irradiation of a “base case” reactive organic gas (ROG) surrogate - NO_x mixture in one of the dual reaction chambers, together with an irradiation, in the other reactor, of the same mixture with the test compound added. The results are analyzed to yield two measures of VOC reactivity: the effect of the added VOC on the amount of NO reacted plus the amount of ozone formed, and integrated OH radical levels. These are discussed in more detail below.

The first measure of reactivity is the effect of the VOC on the change in the quantity [O₃]-[NO], or Δ([O₃]-[NO]). As discussed elsewhere (e.g., Johnson, 1983; Carter and Atkinson, 1987; Carter and Lurmann, 1990, 1991, Carter et al, 1993, 1995a), this gives a direct measure of the amount of conversion of NO to NO₂ by peroxy radicals formed in the photooxidation reactions, which is the process that is directly responsible for ozone formation in the atmosphere. (Johnson calls it “smog produced” or “SP”.) The incremental reactivity of the VOC relative to this quantity, which is calculated for each hour of the experiment, is given by

$$\text{IR}[\Delta([\text{O}_3]-[\text{NO}])_t^{\text{VOC}}] = \frac{\Delta([\text{O}_3]-[\text{NO}])_t^{\text{Test}} - \Delta([\text{O}_3]-[\text{NO}])_t^{\text{Base}}}{[\text{VOC}]_0} \quad (\text{I})$$

where Δ([O₃]-[NO])_t^{Test} is the Δ([O₃]-[NO]) measured at time t from the experiment where the test VOC was added, Δ([O₃]-[NO])_t^{Base} is the corresponding value from the corresponding base case run, and [VOC]₀ is the amount of test VOC added. An estimated uncertainty for IR[Δ([O₃]-[NO])] is derived based on assuming an ~3% uncertainty or imprecision in the measured Δ([O₃]-[NO]) values. This is consistent with the results of the side equivalency test, where equivalent base case mixtures are irradiated on each side of the chamber.

Note that reactivity relative to Δ([O₃]-[NO]) is essentially the same as reactivity relative to O₃ in experiments where O₃ levels are high, because under such conditions [NO]_t^{base} · [NO]_t^{test} · 0, so a change in Δ([O₃]-[NO]) caused by the test compound is due to the change in O₃ alone. However, Δ([O₃]-[NO]) reactivity has the advantage that it provides a useful measure of the effect of the VOC on processes responsible for O₃ formation even in experiments where O₃ formation is suppressed by relatively high NO levels.

The second measure of reactivity is the effect of the VOC on integrated hydroxyl (OH) radical concentrations in the experiment, which is abbreviated as “IntOH” in the subsequent discussion. This is an important factor affecting reactivity because radical levels affect how rapidly all VOCs present, including the base ROG components, react to form ozone. If a compound is present in the experiment that reacts primarily with OH radicals, then the IntOH at time t can be estimated from

$$\text{IntOH}_t = \frac{\ln([\text{tracer}]_0/[\text{tracer}]_t) - Dt}{k\text{OH}^{\text{tracer}}} \quad (\text{II})$$

where $[\text{tracer}]_0$ and $[\text{tracer}]_t$ are the initial and time= t concentrations of the tracer compound, $k\text{OH}^{\text{tracer}}$ its OH rate constant, and D is the dilution rate in the experiments. The latter was found to be small and was neglected in our analysis. The concentration of tracer at each hourly interval was determined by linear interpolation of the experimentally measured values. M-xylene was used as the OH tracer in these experiments because it is a surrogate component present in all experiments, its OH rate constant is known (the value used was $2.36 \times 10^{-11} \text{ cm}^3 \text{ molec}^{-1} \text{ s}^{-1}$ [Atkinson, 1989]), and it reacts relatively rapidly.

The effect of the VOC on OH radicals can thus be measured by its IntOH incremental reactivity, which is defined as

$$\text{IR}[\text{IntOH}]_t = \frac{\text{IntOH}_t^{\text{Test}} - \text{IntOH}_t^{\text{Base}}}{[\text{VOC}]_0} \quad (\text{III})$$

where $\text{IntOH}_t^{\text{Test}}$ and $\text{IntOH}_t^{\text{Base}}$ are the IntOH values measured at time t in the added VOC and the base case experiment, respectively. The results are reported in units of 10^6 min . The uncertainties in IntOH and IR[IntOH] are estimated based on assuming an $\sim 2\%$ imprecision in the measurements of the m-xylene concentrations. This is consistent with the observed precision of results of replicate analyses of this compound.

CHEMICAL MECHANISMS AND MODELING METHODS

Chemical Mechanism

General Atmospheric Photooxidation Mechanism

The chemical mechanism used in the environmental chamber and atmospheric model simulations in this study is the SAPRC-99 mechanism that is documented in detail by Carter (2000). This mechanism represents a complete update of the SAPRC-90 mechanism of Carter (1990), and incorporates recent reactivity data from a wide variety of VOCs, including those discussed in this report. This includes assignments for ~400 types of VOCs, and can be used to estimate reactivities for ~550 VOC categories. A condensed version, developed for use in regional models, is used to represent base case emissions in the atmospheric reactivity simulations discussed in this report. A feature of this mechanism is the use of a computerized system to estimate and generate complete reaction schemes for most non-aromatic hydrocarbons and oxygenates in the presence of NO_x, from which condensed mechanisms for the model can be derived. The SAPRC-99 mechanism was evaluated against the results of almost 1700 environmental chamber experiments carried out at the University of California at Riverside, including experiments to test ozone reactivity predictions for over 80 types of VOCs. This also includes experiments discussed in this report.

A listing of the mechanism as used in the model simulations in this report is given in Appendix A. This consists of the “base mechanism” representing the reactions of the inorganics and common organic products, the reactions of the specific VOCs used in the environmental chamber experiments, and the reactions of the lumped model species used when representing base case VOCs in the ambient reactivity simulations. The report of Carter (2000) should be consulted for a more detailed discussion of these portions of the mechanism. The mechanisms used for the two carbonates studied for this project are discussed below. Note that the mechanisms used for those compounds are the same as used in the report of Carter (2000).

Atmospheric Reactions of Dimethyl Carbonate

The major gas-phase atmospheric loss process for dimethyl carbonate and other carbonates is expected to be reaction with OH radicals. Based on available information for esters and related compounds, reaction with NO₃ radicals (Atkinson, 1991) and O₃ (Atkinson and Carter, 1984; Atkinson, 1994) are expected to be unimportant. The possibility of photolysis can be ruled out on the basis of the absorption cross section data given by Bilde et al (1997), which show no significant absorption at wavelengths above 290 nm. Therefore, only the reaction with OH radicals will be considered in this work.

There are three reported measurements of the rate constant of OH radicals with dimethyl carbonate, with measurements as a function of temperature being made by Bilde et al (1997). Sidebottom et al (1997) and Becker and Sauer (2000) reported rate constants of 3.3×10^{-13} and $3.8 \times 10^{-13} \text{ cm}^3 \text{ molec}^{-1}$

s⁻¹, respectively, at temperatures around 298K. Bilde et al (1997) observed non-Arrhenius temperature dependence, with the rate constant having a minimum around 3.15 x 10⁻¹³ cm³ molec⁻¹ s⁻¹ around 298K, but increasing to 3.3 x 10⁻¹³ and 3.8 x 10⁻¹³ cm³ molec⁻¹ s⁻¹ at 252 and 370K, respectively. For modeling purposes, we use the 298K rate constant of Sidebottom et al (1997), or

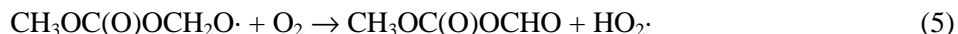
$$k(\text{OH} + \text{Dimethyl Carbonate}) = 3.3 \times 10^{-13} \text{ cm}^3 \text{ molec}^{-1} \text{ s}^{-1}$$

since it is in the middle of the range of the three reported measurements at ambient temperature. This is the rate constant that was used previously when estimating the reactivity of dimethyl carbonate (Carter, 2000), and it was not changed for this work.

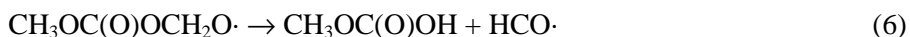
The reaction is expected to proceed by OH abstracting from the methyl group, giving rise in the presence of NO_x in air primarily to CH₃OC(O)OCH₂O· radicals, and perhaps also to a carbonate nitrate



Nitrate formation via Reaction (4) is estimated to be minor because of the relatively small size of the radical combined with the fact that nitrate yields from O-substituted and primary peroxy tend to be lower than those from unsubstituted or secondary peroxy radicals (Carter, 2000). The CH₃OC(O)OCH₂O· radical can react in a number of ways, but according to the SAPRC-99 alkoxy radical estimation methods (Carter, 2000), the dominant processes is expected to be primarily reaction with O₂



or the “ester rearrangement” decomposition, as follows,



This reaction is analogous to the process seen by Tuazon et al (1998) for CH₂CH(O·)OC(O)CH₃ radicals formed from OH + ethyl acetate or by Christensen et al (2000) for CH₃C(O)OCH₂O· radicals formed from OH + methyl acetate.

Based primarily on product data for OH + methyl acetate where the analogous alkoxy + O₂ and ester rearrangement reactions appear to occur at comparable rates, the estimation procedures of Carter (1997), corrected as discussed by Carter et al, 2000b¹, predict that Reaction (5) occurs 1/3 of the time,

¹ The parameters recommended by Carter et al (2000) for estimating ester rearrangement rate constants were in error because of use of an incorrect branching ratio for the products of the methyl acetate + OH reactions when deriving the estimate. This significantly affects only estimates for methyl esters, where reactions forming this radical tend to be relatively unimportant except for the few relatively slowly

with the remaining 2/3 of the reaction being Reaction (6). However, the product data of Bilde et al (1997) suggests that Reaction (5) may be a major process. They observe IR bands attributed to $\text{CH}_3\text{OC}(\text{O})\text{OCHO}$ and derived an estimated yield of ~60% for this product for atmospheric conditions, and did not observe the large yields of the CO expected to be formed following Reaction (6). This estimated 60% yield in fact is consistent with the OH + dimethyl carbonate mechanism previously given by Carter (2000), where it was predicted that Reaction (6) occurred 61% of the time. Therefore, the mechanism given by Carter (2000) was not modified.

Although the branching ratio for the competing reactions of the $\text{CH}_3\text{OC}(\text{O})\text{OCH}_2\text{O}\cdot$ radical is quite uncertain, it should be noted that ozone reactivity predictions for dimethyl carbonate are unaffected by what is assumed in this regard. Both reactions result in a net overall process for the OH + dimethyl carbonate reaction being formation of HO_2 and a relatively inert products (either $\text{CH}_3\text{OC}(\text{O})\text{OCHO}$ or $\text{CH}_3\text{OC}(\text{O})\text{OH} + \text{CO}$) after the conversion of one molecule of NO to NO_2 . The different products react so slowly that their contribution to the overall reactivity of dimethyl carbonate in a 6-hour chamber experiment or a one-day atmospheric simulation would be negligible.

In terms of model species used in the SAPRC-99 mechanism, the overall reaction of OH with dimethyl carbonate (DMC) is given as follows:



Here the $\text{RO}_2\text{-R}\cdot$ represents the formation of peroxy radicals that react to convert NO to NO_2 and form HO_2 , RCO-OH represents lumped higher organic acids ($\text{CH}_3\text{OC}(\text{O})\text{OH}$ in this case), and INERT is used to represent $\text{CH}_3\text{OC}(\text{O})\text{OCHO}$, which is estimated to react relatively. This mechanism is essentially the same as that used by Carter (2000), so that mechanism was used in all the model simulations for this compound used in this work².

Atmospheric Reactions of Methyl Isopropyl Carbonate

As is the case with dimethyl carbonate, methyl isopropyl carbonate is expected to react primarily with OH radicals. Unlike dimethyl carbonate, no information could be found in the literature concerning

reacting methyl esters such as methyl acetate or dimethyl carbonate. The corrected derivation is as follows. The A factor assumed to be approximately the same as assumed for 1,4-H-shift isomerizations, based on expected similarities in transition states, and is the same as used by Carter (2000). The activation energies are assumed to be linearly dependent on the heat of reaction, where $E_a = E_{aA} + E_{aB} \times \Delta H_r$, and $E_{aA} = 9.11$ and $E_{aB} = 0.20$ were derived to be consistent with OH + methyl acetate product yields reported by Christensen et al (2000), OH + ethyl acetate yields of Tuazon et al (1998), and results of modeling n-butyl acetate reactivity chamber experiments.

² Using the ester rearrangement rate constant estimate that turned out to be based on incorrect data, the methyl acetate mechanism derived by Carter (2000) had a 61% yield of "INERT" and 39% yields of "CO and RCO-OH". The difference between this and the recommended mechanism is too small to merit changing the mechanism used in the previous work.

this reaction. Therefore, the OH radical rate constant was measured in this work, and as discussed later in this report it was determined to be

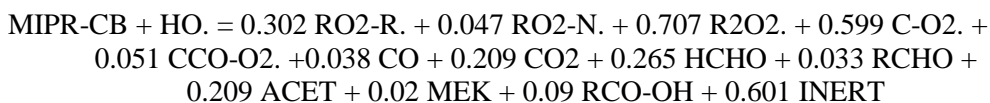
$$k(\text{OH} + \text{Methyl Isopropyl Carbonate}) = 2.55 \times 10^{-12} \text{ cm}^3 \text{ molec}^{-1} \text{ s}^{-1}$$

at ~295 - 300°K and atmospheric pressure. The estimated uncertainty is $\pm 25\%$. This is about 30% less than the rate constant of $3.66 \times 10^{-12} \text{ cm}^3 \text{ molec}^{-1} \text{ s}^{-1}$ that is estimated using the group additivity method of Kwok and Atkinson (1995), which is well within the uncertainty of the estimation method.

There is no information available concerning the mechanism for the OH reaction, so an estimated mechanism derived using the SAPRC-99 mechanism estimation and generation system (Carter, 2000) is used. The detailed mechanism for the reactions in the presence of NO_x as derived using this system is given in Table 1, where footnotes briefly indicate the estimation procedures that were used (see Carter, 2000 for details). The table also gives the estimated branching ratios for the competitive reactions involved, and the relative contributions of each reaction to the total methyl isopropyl carbonate photooxidation process. Reactions that contribute less than 1% are not shown.

Although there is some reaction at the other positions of the molecule, most of the reaction of OH with methyl isopropyl carbonate is estimated to be at the tertiary hydrogen, ultimately resulting in the formation of $\text{CH}_3\text{C}(\text{O}\cdot)(\text{CH}_3)\text{OC}(\text{O})\text{OCH}_3$ radicals and the corresponding alkyl nitrate. About 3/4 of this is estimated to decompose to methyl radicals (which ultimately form formaldehyde and HO_2 after an NO to NO_2 conversion) and $\text{CH}_3\text{OC}(\text{O})\text{OC}(\text{O})\text{CH}_3$. The remaining 1/4 of this alkoxy radical is estimated to decompose to form acetone and a carbonate radical that ultimately decomposes and reacts to form CO_2 and additional formaldehyde. Thus the major predicted products are formaldehyde, $\text{CH}_3\text{OC}(\text{O})\text{OC}(\text{O})\text{CH}_3$, acetone, and CO_2 , with the formaldehyde / acetone + CO_2 yield ratio depending on the ratio of competing decompositions of the $\text{CH}_3\text{C}(\text{O}\cdot)(\text{CH}_3)\text{OC}(\text{O})\text{OCH}_3$ radical, which is quite uncertain. Although a comprehensive product study was not carried out as part of this work, acetone was observed as a product in the reactivity chamber experiments at approximately the levels predicted by this mechanism.

As discussed below, the estimated mechanism given in Table 1 gave sufficiently good simulations of the environmental chamber reactivity experiments that it was used without adjustment. In terms of SAPRC-99 model species, this OH + methyl isopropyl carbonate (MIPR-CB) mechanism is given by



Here the $\text{RO}_2\text{-R}\cdot$ represents the formation of peroxy radicals that react to convert NO to NO_2 and form HO_2 , $\text{RO}_2\text{-N}\cdot$ represents the formation of peroxy radicals that react with NO to form organic nitrates, $\text{R}_2\text{O}_2\cdot$ represents extra NO to NO_2 conversions caused by peroxy radicals formed in multi-step mechanisms, $\text{CCO-O}_2\cdot$ represents $\text{CH}_3\text{C}(\text{O})\text{OO}\cdot$ radicals, RCHO represents the lumped higher aldehyde [$\text{CH}_3\text{CH}(\text{CHO})\text{OC}(\text{O})\text{OCH}_3$ in this case], ACET represents acetone, MEK represents the lumped lower

Table 1. Detailed mechanism for the reactions of OH radicals with methyl isopropyl carbonate as generated using the SAPRC-99 mechanism generation system, with corrected estimates for ester rearrangement reactions.

Reactions	Notes [a]	Yields		
		Rxn	Total	
<u>CH₃CH(CH₃)OC(O)OCH₃</u>				
1	+ OH → H ₂ O + CH ₃ CH(CH ₂ ·)OC(O)OCH ₃	1	9%	9%
2	+ OH → H ₂ O + CH ₃ C(·)(CH ₃)OC(O)OCH ₃	1	85%	85%
3	+ OH → H ₂ O + CH ₃ CH(CH ₃)OC(O)OCH ₂ ·	1	6%	6%
<u>Radicals Formed from Reaction at the Isopropyl Methyl Group</u>				
4	CH ₃ CH(CH ₂ ·)OC(O)OCH ₃ + O ₂ → CH ₃ CH(CH ₂ OO·)OC(O)OCH ₃			9%
5	CH ₃ CH(CH ₂ OO·)OC(O)OCH ₃ + NO → NO ₂ + CH ₃ CH(CH ₂ O·)OC(O)OCH ₃	2	95%	9%
6	+ NO → CH ₃ CH(CH ₂ ONO ₂)OC(O)OCH ₃	2	5%	<1%
7	CH ₃ CH(CH ₂ O·)OC(O)OCH ₃ + O ₂ → CH ₃ CH(CHO)OC(O)OCH ₃ + HO ₂ ·	3	37%	3%
8	→ HCHO + CH ₃ OC(O)OCH(·)CH ₃	3	63%	6%
9	CH ₃ OC(O)OCH(·)CH ₃ + O ₂ → CH ₃ OC(O)OCH(OO·)CH ₃			6%
10	CH ₃ OC(O)OCH(OO·)CH ₃ + NO → NO ₂ + CH ₃ OC(O)OCH(O·)CH ₃			5%
11	CH ₃ OC(O)OCH(O·)CH ₃ → CH ₃ OC(O)OH + CH ₃ C(O)·	3,4,5		5%
12	CH ₃ C(O)· + O ₂ → CH ₃ C(O)OO·			5%
<u>Radicals Formed from Reaction at the Isopropyl Tertiary Hydrogen</u>				
13	CH ₃ C(·)(CH ₃)OC(O)OCH ₃ + O ₂ → CH ₃ C(OO·)(CH ₃)OC(O)OCH ₃			85%
14	CH ₃ C(OO·)(CH ₃)OC(O)OCH ₃ + NO → CH ₃ C(CH ₃)(ONO ₂)OC(O)OCH ₃	3	5%	4%
15	+ NO → NO ₂ + CH ₃ C(O·)(CH ₃)OC(O)OCH ₃		96%	81%
16	CH ₃ C(O·)(CH ₃)OC(O)OCH ₃ → CH ₃ OC(O)OC(O)CH ₃ + CH ₃ ·	3	74%	60%
17	→ CH ₃ C(O)CH ₃ + CH ₃ OC(O)O·	3	26%	21%
18	CH ₃ · + O ₂ → CH ₃ OO·			60%
19	CH ₃ OO· + NO → NO ₂ + CH ₃ O·			60%
20	CH ₃ OC(O)O· → CO ₂ + CH ₃ O·	6		21%
21	CH ₃ O· + O ₂ → HCHO + HO ₂ ·			81%
<u>Radicals Formed from Reaction at the Methoxy Group</u>				
22	CH ₃ CH(CH ₃)OC(O)OCH ₂ · + O ₂ → CH ₃ CH(CH ₃)OC(O)OCH ₂ OO·			6%
23	CH ₃ CH(CH ₃)OC(O)OCH ₂ OO· + NO → NO ₂ + CH ₃ CH(CH ₃)OC(O)OCH ₂ O·	2	95%	6%
24	+ NO → CH ₃ CH(CH ₃)OC(O)OCH ₂ ONO ₂	2	5%	<1%
25	CH ₃ CH(CH ₃)OC(O)OCH ₂ O· + O ₂ → CH ₃ CH(CH ₃)OC(O)OCHO + HO ₂ ·	3	34%	2%
26	→ CH ₃ CH(CH ₃)OC(O)OH + HCO·	5	66%	4%
27	HCO· + O ₂ → CO + HO ₂ ·			4%

Table 1 (continued)

- [a] Documentation notes for branching ratios are as follows. See Carter (2000) for details concerning the estimation methods.
- 1 Branching ratio derived using the group additivity method of Kwok and Atkinson (1995).
 - 2 The branching ratio for nitrate formation (nitrate yield) is using the procedures of Carter (2000), based on yields derived for other compounds.
 - 3 Rate constants for alkoxy radical reactions estimated as discussed by Carter (2000).
 - 4 The ester rearrangement is estimated to be the major reaction route
 5. Estimation method for ester rearrangement rate constant corrected as discussed in the text.
 - 6 This decomposition is assumed to be fast.
- [c] Predicted branching ratios. The “Rxn” column shows the importance of the reaction relative to the competing reactions of the species or radical. The “Total” column show the importance of the reaction relative to the overall process.

reactivity non-aldehyde oxygenated product [$\text{CH}_3\text{CH}(\text{CH}_3)\text{OC}(\text{O})\text{OCHO}$ in this case], RCO-OH represents lumped higher organic acids [$\text{CH}_3\text{OC}(\text{O})\text{OH}$ and $\text{CH}_3\text{CH}(\text{CH}_3)\text{OC}(\text{O})\text{OH}$ in this case], and INERT is used to represent primarily dimethyl carbonate, which has sufficiently low reactivity that its contribution to the product reactivity is negligible. The OH rate constant used is that determined in this work as indicated above. This mechanism is used in all the model simulations discussed in this report.

Modeling Methods

Environmental Chamber Simulations

The ability of the chemical mechanisms to appropriately simulate the atmospheric impacts of methyl carbonate and methyl isopropyl carbonate were evaluated by conducting model simulations of the environmental chamber experiments carried out for this study. This requires including in the model appropriate representations of chamber-dependent effects such as wall reactions and characteristics of the light source. The methods used are based on those discussed in detail by Carter and Lurmann (1990, 1991), updated as discussed by Carter et al. (1995c; 1997, 2000a). The photolysis rates were derived from results of NO_2 actinometry experiments and measurements of the relative spectra of the light source. The thermal rate constants were calculated using the temperatures measured during the experiments, with the small variations in temperature with time during the experiment being taken into account. The computer programs and modeling methods employed are discussed in more detail elsewhere (Carter et al, 1995c). The specific values of the chamber-dependent parameters used in the model simulations of the experiments for this study are given in Table A-4 in Appendix A.

In the case of the carbonates studied for this project, all model calculations used the mechanisms as discussed in the previous section without adjustments or modifications. They are the same as those used by Carter (2000), and are included in the listing on Appendix A.

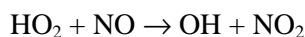
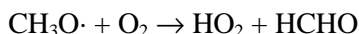
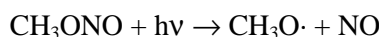
Atmospheric Reactivity Simulations

To estimate their effects on ozone formation under conditions more representative of polluted urban atmospheres, incremental reactivities, defined as the change in O₃ caused by adding small amounts of the compound to the emissions, were calculated for the two carbonates, as well as for ethane and other representative compounds. The scenarios employed are discussed in more detail later in this report, and are the same as used in our previous studies (Carter 1994a,b, 2000). The, software, and calculation procedures are as described by Carter (1994b), and were exactly the same as used by Carter (2000) when calculating the reactivity scale for the SAPRC-99 mechanism. The mechanism used is given in Appendix A.

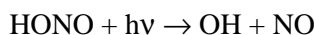
EXPERIMENTAL AND MECHANISM EVALUATION RESULTS

Relative Rate Constant Measurements

The rate constants for the reactions of OH radicals with methyl isopropyl carbonate and (for control purposes) n-butane and benzene were measured using a relative rate method, with propane used as the reference compound. The relative rate method employed has been used extensively in other laboratories for many years [see references cited by Atkinson (1989), e.g., Atkinson et al, 1981)], and involves measurements of the consumption of the various compounds in the presence of OH radicals. In this work, the OH radicals were generated either by the photolysis of methyl nitrite



or by the photolysis of nitrous acid



Excess NO is added when methyl nitrite is used as the radical source to avoid the formation of O₃ and NO₃ radicals. This is not necessary in the experiments using HONO as the radical source since NO is formed in the photolysis of HONO.

Assuming that the organics react only with OH radicals, the kinetic differential equations for the organics can be solved and rearranged to yield

$$\ln\left(\frac{[\text{Organic}]_{t0}}{[\text{Organic}]_t}\right) - D_t = \frac{k_{\text{Organic}}}{k_{\text{Reference}}}\ln\left[\left(\frac{[\text{Reference}]_{t0}}{[\text{Reference}]_t}\right) - D_t\right] \quad (\text{IV})$$

where [Organic]_{t0} and [Organic]_t, [Reference]_{t0}, and [Reference]_t are the initial and time=t concentrations of the test and reference compounds, respectively, k_{Organic} and k_{Reference} are the test and reference compound's OH rate constant, and D_t is a factor added to account for dilution due to reactant injections, leaks, etc, from the beginning of the experiment up to time t. Since no reactant injections were made during the experiments and the leaks in this chamber are believed to be negligible during the time period of the experiments, D_t is assumed to be negligible in our analysis. Therefore plots of ln([Organic]_{t0}/[Organic]_t) against ln([Reference]_{t0}/[Reference]_t) should yield a straight line with intercept of approximately zero and a slope that is the ratio of rate constants. Given the known value of k_{Reference}, then k_{Organic} can then be derived. In principle all of the compounds could be present in the same experiment but because of GC interferences and other factors generally only 2-4 test compounds are present in any given experiment.

To verify the method as employed in this study, relative rate constants were also determined for n-butane and benzene, for comparison with literature results. N-Butane was used for verification purposes because its OH radical rate constant is well established. Benzene was also used because of possible concern that HCl may be an impurity in the HONO generator, since it is used in the synthesis of HONO, and if present it could result in possible introduction of Cl atoms in the system. Although the rate constants for the reactions of OH radicals with propane and benzene are very similar, Cl atoms reacts rapidly with propane [$k = 1.37 \times 10^{-10} \text{ cm}^3 \text{ molec}^{-1} \text{ s}^{-1}$ (Atkinson, 1997)] but very slowly with benzene [$k = (1.3 - 1.5) \times 10^{-15} \text{ cm}^3 \text{ molec}^{-1} \text{ s}^{-1}$ (Atkinson and Aschmann, 1985; Shi and Bernhard, 1997)]. Therefore, if there were significant consumption of reactants with Cl atoms, the apparent OH radical rate constant for benzene using propane as the reference compound would be low.

Six kinetic experiments were carried out for this project, and their conditions and detailed measurement data are given on Table 2. Plots of Equation (IV) are shown on Figure 1 for each of the four test compounds. Note that the initial reactant concentrations used when deriving these plots were determined using a least squares optimization method to minimize least squares errors in fits of the data to Equation (IV), with the initial reactant concentrations as well as the ratios of rate constants being simultaneously optimized during this process. This procedure minimizes biases introduced by experimental uncertainties in the initial reactant measurements, and allows all of the measurements to be weighted equally when determining rate constant ratios according to Equation (IV). The results are summarized on Table 3.

Figure 1 shows that excellent precision was obtained in the measurements of the relative rate constants for n-butane and benzene, and fair precision was obtained in the relative rate measurements with methyl isopropyl carbonate. The rate constant ratios derived from the separate experiments had standard deviations of 3%, 8%, and 16% for n-butane, benzene, and methyl isopropyl carbonate, respectively. The lower precision for the test compounds is apparently due to lower precision in analysis of the oxygenated compounds relative to the hydrocarbons. This is seen in replicate analyses of unreacting mixtures in the dark.

The rate constants determined in this work for n-butane and benzene are in good agreement with the literature values, suggesting that there are no systematic problems in our measurements. Note that the OH + benzene rate constant determined in this work is slightly higher than the previously determined values, which is the opposite direction of the discrepancy that would be expected if Cl atoms were reacting in the system. There were no significant differences between the experiments where HONO was used as the OH radical source compared to those where methyl nitrite was used.

Based on these data, we conclude that the rate constant for the reaction of OH radicals with methyl isopropyl carbonate is $2.55 \times 10^{-12} \text{ cm}^3 \text{ molec}^{-1} \text{ s}^{-1}$, with an estimated uncertainty of around $\pm 25\%$. We are not aware of any previous measurement of this rate constant.

Table 2. Summary of conditions and measurement data for the kinetic experiments carried out for this program.

	Propane	n-Butane	Benzene	Methyl Isopropyl Carbonate
	Run 1. 6/8/99. Pillow Bag. 1-2 ppm HONO			
Init.	0.147	0.150	0.181	0.133
Init.	0.148	0.150	0.181	0.130
Init.	0.146	0.149	0.180	0.136
	0.143	0.141	0.175	0.128
	0.142	0.140	0.176	0.129
	0.136	0.127	0.168	0.115
	0.135	0.126	0.168	0.115
	0.130	0.117	0.162	0.107
	0.133	0.119	0.163	0.104
	0.129	0.113	0.160	0.103
	0.130	0.114	0.160	0.102
	0.129	0.111	0.159	0.103
	0.129	0.113	0.161	0.105
	0.128	0.109	0.158	0.102
	Run 2. 6/18/99. Pillow Bag. 1-2 ppm HONO			
Init.	0.169	0.191	0.170	0.177
Init.	0.168	0.190	0.168	0.177
	0.161	0.177	0.161	0.159
	0.162	0.177	0.163	0.164
	0.158	0.166	0.158	0.150
	0.158	0.167	0.158	0.152
	0.152	0.155	0.154	0.145
	0.154	0.156	0.154	0.141
	0.148	0.148	0.149	0.135
	0.150	0.147	0.151	0.133
	0.148	0.144	0.149	0.133
	0.146	0.139	0.147	0.126
	0.145	0.139	0.147	0.129
	0.145	0.137	0.146	0.127
	0.145	0.140	0.146	0.128
	Run 3. 6/30/99. Pillow Bag. ~2 ppm Methyl Nitrite. ~3 ppm NO			
Init.	0.341		0.326	0.385
Init.	0.351		0.338	0.438
Init.	0.348		0.338	0.450
	0.343		0.330	0.417
	0.343		0.330	0.423
	0.326		0.318	0.369
	0.322		0.314	0.370
	0.325		0.315	0.366
	0.319		0.314	0.353
	0.317		0.310	0.354
	0.312		0.306	0.348
	0.314		0.309	0.343
	0.308		0.303	0.341
	0.303		0.299	0.331

Table 2 (continued)

	Propane	n-Butane	Benzene	Methyl Isopropyl Carbonate
	0.302		0.298	0.315
	0.302		0.296	0.320
	0.296		0.295	0.314
	0.299		0.300	0.316
	0.303		0.299	0.331
	0.300		0.300	0.331
	Run 4. 7/2/99. Pillow Bag. ~2 ppm Methyl Nitrite. ~2 ppm NO			
Init.	0.245	0.371	0.346	0.563
Init.	0.246	0.371	0.344	0.532
	0.236	0.346	0.332	0.454
	0.237	0.351	0.332	0.462
	0.231	0.328	0.325	0.435
	0.230	0.323	0.322	0.408
	0.222	0.302	0.312	0.382
	0.226	0.306	0.319	0.396
	0.219	0.293	0.310	0.393
	0.217	0.291	0.307	0.380
	0.219	0.290	0.306	0.371
	0.220	0.293	0.307	0.373
	0.218	0.289	0.307	0.361
	0.217	0.287	0.306	0.358
	0.211	0.272	0.297	0.346
	0.209	0.269	0.296	0.335
	Run 5. 7/8/99. DTC789. ~2 ppm Methyl Nitrite. ~3 ppm NO			
Init.	0.311	0.336	0.273	0.357
Init.	0.315	0.343	0.279	0.398
Init.	0.312	0.340	0.275	0.381
Init.	0.312	0.340	0.278	0.413
	0.308	0.333	0.273	0.382
	0.307	0.329	0.274	0.381
	0.307	0.325	0.273	0.379
	0.305	0.324	0.272	0.374
	0.299	0.313	0.267	0.355
	0.301	0.313	0.266	0.352
	0.293	0.296	0.261	0.334
	0.295	0.299	0.260	0.328
	0.291	0.292	0.258	0.317
	0.285	0.281	0.257	0.324
	0.289	0.284	0.257	0.331
	0.284	0.276	0.254	0.324
	0.283	0.276	0.252	0.316
	0.281	0.272	0.250	0.303
	0.278	0.269	0.250	0.310
	Run 6. 7/13/99. Pillow Bag. 1-2 ppm HONO			
Init.	0.110	0.112	0.111	0.126
Init.	0.109	0.109	0.112	0.133
Init.	0.110	0.112	0.112	0.138

Table 2 (continued)

Propane	n-Butane	Benzene	Methyl Isopropyl Carbonate
0.108	0.105	0.109	0.126
0.107	0.107	0.111	0.130
0.102	0.095	0.105	0.112
0.102	0.094	0.106	0.112
0.099	0.090	0.103	0.105
0.101	0.091	0.104	0.110
0.100	0.091	0.103	0.105
0.099	0.089	0.103	0.104
0.099	0.087	0.102	0.097
0.097	0.086	0.102	0.100
0.096	0.082	0.100	0.095
0.093	0.079	0.097	0.092
0.092	0.077	0.096	0.089
0.091	0.077	0.096	0.088
0.090	0.075	0.095	0.088

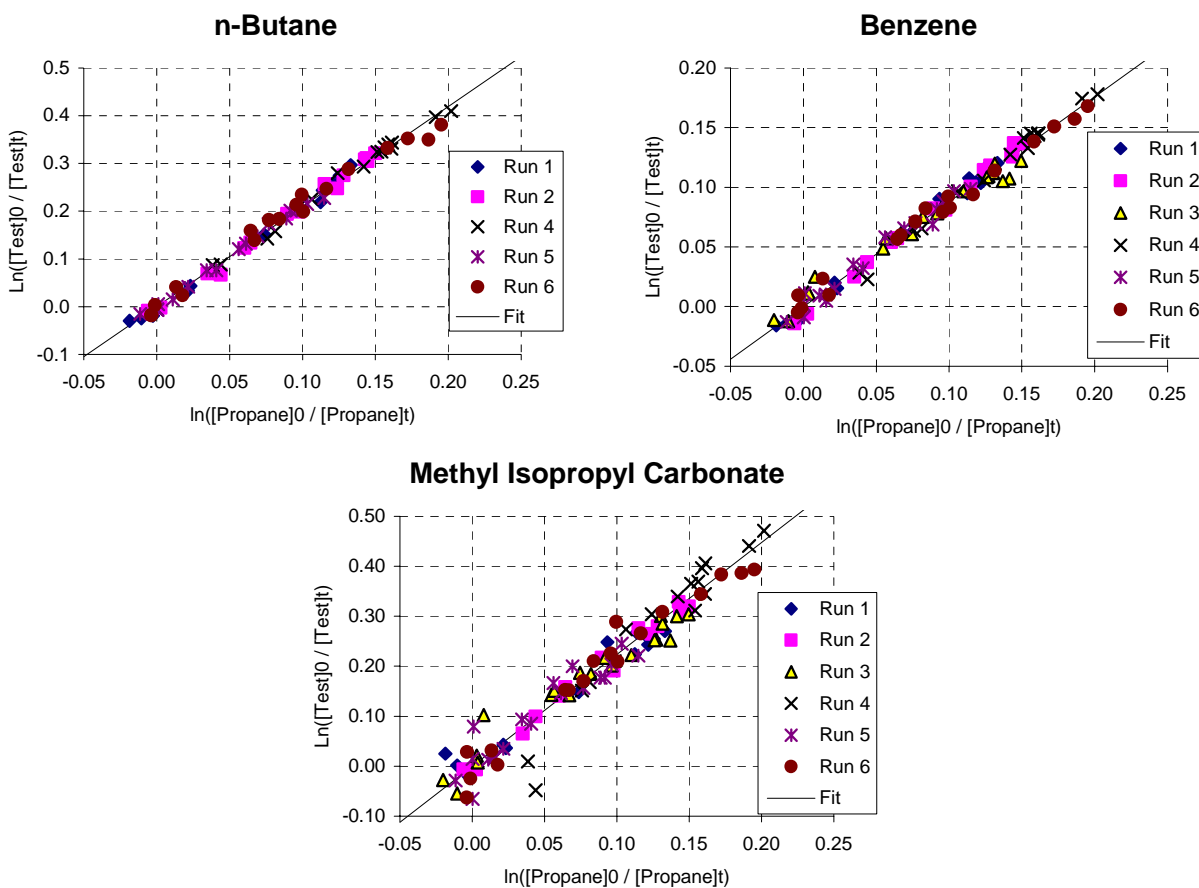


Figure 1. Plots of Equation (IV) for n-butane, benzene, and methyl isopropyl carbonate, with propane as the test compound.

Table 3. Summary of Results of OH Radical Rate Constant Measurements.

Compound	kOH / kOH (Propane) [a]	kOH (cm ³ molec ⁻¹ s ⁻¹)		
		This Work [b]	Literature	Reference
n-Butane	2.10 ± 0.08	2.39 x 10 ⁻¹²	2.47 x 10 ⁻¹²	Atkinson (1997)
Benzene	0.88 ± 0.08	1.00 x 10 ⁻¹²	1.23 x 10 ⁻¹²	Atkinson (1989)
Methyl Isopropyl Carbonate	2.24 ± 0.38	2.55 x 10 ⁻¹²	-	

[a] Rate constant ratio determined to minimize least squares errors between $\ln([\text{VOC}]_0/[\text{VOC}]_t)$ calculated using Equation (IV) and the experimentally measured values. The initial propane and test VOC concentrations in each experiment were also optimized as part of this determination, to avoid biases introduced by uncertainties in initial reactant concentrations used in Equation (IV). Dilution is assumed to be negligible in all experiments. The stated error limits reflect precision on measurement only and are estimated based on variation in rate constant ratios obtained from the various experiments.

[b] Placed on an absolute basis using kOH for propane of $1.14 \times 10^{-12} \text{ cm}^3 \text{ molec}^{-1} \text{ s}^{-1}$ at 298K.

Summary of Environmental Chamber Experiments and Characterization Results

Table 4 gives a chronological listing of all the experiments carried out for this program. These consisted primarily of the experiments with the two carbonates, which are discussed in the next section. In addition to these, several characterization runs were carried out to determine the chamber-dependent inputs needed for the model simulations of the experiments. Table 4 summarizes the purposes and relevant results from these runs.

As indicated on Table 4, the results of most of these experiments were as expected based on our previous experience with these and similar chambers in our laboratories (Carter et al, 1995c and references therein; Carter et al, 2000a), and indicated no special problems when characterizing run conditions for mechanism evaluation. See Carter et al (2000a) for more discussion of the characterization results for these chambers during this time period, particularly with respect to light intensity and the chamber radical source. As noted on the table, some experiments were carried out following experiments where small amounts (usually less than 100 ppb) of nitrous acid was injected into the chamber, and there was initially some concern that this might affect some experiments. However, with one exception no unusual results were found in characterization tests such as n-butane - NO_x irradiations (which are sensitive to the chamber radical source) that followed such experiments. The one exception was an apparent contamination with a Cl atom source in an experiment where relatively large amounts of HONO were injected into the chamber during the period just before the methyl isopropyl carbonate experiments. However, after conditioning, normal results were obtained in a butane - NO_x run carried out before the first methyl isopropyl carbonate run (see comments for DTC745 on Table 4).

Table 4. Chronological listing of the environmental chamber experiments carried out for this program.

Run ID	Date	Title	Comments
DTC673	6/22/98	NO ₂ Actinometry	NO ₂ photolysis rate measured using the quartz tube method was 0.156 min ⁻¹ , in good agreement with the trend observed with the other such runs.
DTC682	7/8/98	Ozone and CO dark Decay	Control run to check for leaks and measure the O ₃ wall decay rate. Essentially no CO decay was observed, indicating negligible leakage. The O ₃ decay rates were 1.4 x 10 ⁻⁴ min ⁻¹ on Side A and 1.6 x 10 ⁻⁴ min ⁻¹ on Side B, in excellent agreement with the value of 1.5 x 10 ⁻⁴ min ⁻¹ that is used when modeling these DTC runs.
DTC683	7/9/98	Propene - NO _x	Standard propene - NO _x control run for comparison with other such runs in this and other chambers. Results in normal range.
DTC684	7/13/98	NO ₂ Actinometry	NO ₂ photolysis rate measured using the quartz tube method was 0.160 min ⁻¹ , in good agreement with the trend observed with the other such runs.
	7/20 - 7/31/98	Runs for another program	Runs were carried out for other programs that involved injections of sub-ppm amounts of HONO in the chamber. Tests carried out in separate experiments indicate that this shouldn't affect the results of subsequent experiments.
DTC691	8/4/98	Mini-Surrogate + Dimethyl Carbonate attempt.	An attempt to carry out a mini-surrogate experiment with dimethyl carbonate added to Side B had to be aborted because of experimental problems.
DTC692	8/6/98	Mini-Surrogate + Dimethyl Carbonate	Mini-surrogate reactivity experiment with 24 ppm dimethyl carbonate added to Side B. Results on Table 5 and Figure 3
DTC693	8/7/98	Full Surrogate + Dimethyl Carbonate	High NO _x full surrogate reactivity experiment with 21 ppm dimethyl carbonate added to Side A. Results on Table 5 and Figure 3
	8/12 - 8/18/98	Runs for other programs	Runs were carried out for other programs. One other experiment involved injections of sub-ppm amounts of HONO in the chamber.
DTC698	8/19/98	Low NO _x Full Surrogate + Dimethyl Carbonate (B)	Low NO _x full surrogate reactivity experiment with 21 ppm dimethyl carbonate added to Side A. Results on Table 5 and Figure 3
DTC699	8/20/98	n-Butane - NO _x	Characterization run to measure the chamber radical source. The NO oxidation rates were consistent with those predicted by the standard chamber model, but the rate on Side B was slightly higher than that on Side A.
	8/21 - 8/27/98	Runs for another program	
DTC703	8/28/98	Mini-Surrogate + Dimethyl Carbonate	Mini-surrogate reactivity experiment with 41 ppm dimethyl carbonate added to Side B. Results on Table 5 and Figure 3
DTC704	8/31/98	NO ₂ Actinometry	NO ₂ photolysis rate measured using the quartz tube method was 0.165 min ⁻¹ , in good agreement with the trend observed with the other such runs.

Table 4 (continued)

Run ID	Date	Title	Comments
DTC705	9/1/98	Full Surrogate + Dimethyl Carbonate	High NO _x full surrogate reactivity experiment with 16 ppm dimethyl carbonate added to Side A. Results on Table 5 and Figure 3
DTC706	9/2/98	Propene - NO _x	Standard propene - NO _x control run for comparison with other such runs in this and other chambers. Results in normal range.
	9/3/98	Run for another program	
DTC708	9/4/98	Low NO _x Full Surrogate Side equivalence Test	Irradiation of the same low NO _x full surrogate mixture was carried out in both reactors to determine side equivalency for this type of experiment. The NO oxidation rates and initial O ₃ formation rates were the same on both sides, but the maximum ozone was slightly less on Side B, and the O ₃ decayed slightly faster on that side once the peak O ₃ concentration was reached. The maximum and final O ₃ on side A was around 265 ppb, and the maximum O ₃ on side B was around 250 ppb after 3 hours, declining to ~230 ppb at the end of the 6-hour run. N-Butane data suggest a slightly higher than normal leak rate on Side B, but it was still less than 1% per hour.
DTC709	9/8/98	Ozone and CO dark Decay	Control run to check for leaks and measure the O ₃ wall decay rate just before replacing the reaction bat. Essentially no CO decay was observed, indicating negligible leakage. The O ₃ decay rates were 1.2 x 10 ⁻⁴ min ⁻¹ on Side A and 2.1 x 10 ⁻⁴ min ⁻¹ in Side B, in fair agreement with the value of 1.5 x 10 ⁻⁴ min ⁻¹ that is used when modeling these DTC runs. The higher decay rate in Side B is consistent with the results of run DTC708. However, changing the O ₃ wall loss rate within this range does not significantly affect results of model simulations of this run.
DTC710	10/19/98	n-Butane - NO _x	Run to measure the rate of the chamber radical source, as discussed by Carter et al (1995c). Results are well simulated using the standard chamber model assigned to this series of experiments, and good side equivalency was obtained.
DTC711	10/20 - 10/30/98	Runs for another program	Some of the runs carried out involved injections of sub-ppm amounts of HONO in the chamber. Tests carried out in separate experiments indicate that this shouldn't affect the results of subsequent experiments.
DTC718	10/30/98	n-Butane - NO _x	Run to measure the rate of the chamber radical source, as discussed by Carter et al (1995c). The NO oxidation rate was slightly higher on Side A, but the results were in the normal range and were well simulated using the standard chamber model assigned to this series of experiments.
	11/4 - 12/8/98	Runs for other projects.	

Table 4 (continued)

Run ID	Date	Title	Comments
	12/10 - 12/14/98	kOH Determination with HONO	Runs for another program caused contamination with HONO and/or HCl. Replicate n-butane runs were carried out until normal NO oxidation rates were observed.
DTC745	12/14/98	n-Butane - NO _x	Run to measure the rate of the chamber radical source after the chamber contamination and reconditioning procedure. The NO oxidation rates on both sides were somewhat lower than predicted by the standard chamber model, but the results were in the normal range. Since the contamination should cause higher than normal NO oxidation rates, it is concluded that the chamber has been adequately reconditioned.
	12/15 - 12/18/98	Runs for another program	
DTC750	12/19/98	Mini-Surrogate + Methyl Isopropyl Carbonate	Mini-surrogate reactivity experiment with 4.5 ppm dimethyl carbonate added to Side B. Results on Table 5 and Figure 4
DTC751	12/22/98	n-Butane - Chlorine Actinometry	Run to measure the light intensity by determining the Cl ₂ photolysis rate, as discussed by Carter et al (1995c). The results yielded a calculated NO ₂ photolysis rate of 0.153 min ⁻¹ , which is reasonably consistent with the results of the quartz tube Actinometry experiments carried out previously, which indicated an NO ₂ photolysis rate of ~0.16 min ⁻¹ .
DTC752	1/5/99	n-Butane - NO _x	Run to measure the rate of the chamber radical source, as discussed by Carter et al (1995c). Results are reasonably well simulated using the standard chamber model assigned to this series of experiments (see Table A-4), though Side B has a somewhat higher radical source than Side A.
	1/6 - 1/7/99	Runs for another program	
DTC755	1/8/99	Full Surrogate + Methyl Isopropyl Carbonate	High NO _x full surrogate reactivity experiment with 3.1 ppm dimethyl carbonate added to Side A. Results on Table 5 and Figure 4
	1/11 - 1/23/99	Runs for another program	
DTC758	1/13/99	Low NO _x Full Surrogate + Methyl Isopropyl Carbonate	Low NO _x full surrogate reactivity experiment with 3.3 ppm dimethyl carbonate added to Side B. Results on Table 5 and Figure 4
DTC759	1/14/99	Mini-Surrogate + Methyl Isopropyl Carbonate	Mini-surrogate reactivity experiment with 3.8 ppm dimethyl carbonate added to Side A. Results on Table 5 and Figure 4
	1/15/99	Run for another program	
DTC761	1/20/99	Propene - NO _x	Standard propene - NO _x control run for comparison with other such runs in this and other chambers. Results in normal range.

Table 4 (continued)

Run ID	Date	Title	Comments
DTC762	1/21/99	Full Surrogate + Methyl Isopropyl Carbonate	High NO _x full surrogate reactivity experiment with 1.7 ppm dimethyl carbonate added to Side A. Results on Table 5 and Figure 4
DTC763	1/22/99	Low NO _x Full Surrogate + Methyl Isopropyl Carbonate	Low NO _x full surrogate reactivity experiment with 1.6 ppm dimethyl carbonate added to Side B. Results on Table 5 and Figure 4
DTC764	1/26/99	Acetaldehyde + air	Run to test for NO _x wall offgasing effects. Approximately 17 ppb of O ₃ and 4 ppb of PAN formed after six hours of irradiation, with similar results on both sides. Results in good agreement with predictions of standard chamber wall model.
DTC765	2/2 - 2/5/99	Runs for another program.	
DTC767	2/8/99	n-Butane - NO _x	Run to measure the rate of the chamber radical source. Results are simulated very well using the standard chamber model assigned to this series of experiments (see Table A-4), and good side equivalency is observed. This indicates that that the magnitude of the chamber radical source is in the normal range, and that the side differences observed in DTC752 are no longer occurring.
DTC768	2/9 - 2/17/99	Run for other programs.	
DTC774	2/19/99	n-Butane - Chlorine Actinometry.	Run to measure the light intensity by determining the Cl ₂ photolysis rate, as discussed by Carter et al (1995c). The results yielded a calculated NO ₂ photolysis rate of 0.105 min ⁻¹ , which lower than indicated by the results of the quartz tube actinometry experiments, which indicate an NO ₂ photolysis rate of ~0.16 min ⁻¹ . However, the results of these Cl ₂ experiments in this chamber tend to be scattered, and this discrepancy is not outside of the range of this variability. The results were not used for assigning NO ₂ photolysis rates for modeling.
DTC789	2/22 - 7/7/99 7/8/99	Runs for other programs Kinetic Experiment for Methyl Isopropyl Carbonate	The irradiation of methyl nitrite in the presence of NO was used as the OH radical source to determine the relative rate constants for the reactions of OH radicals with propane, n-butane, and benzene. See text for results.

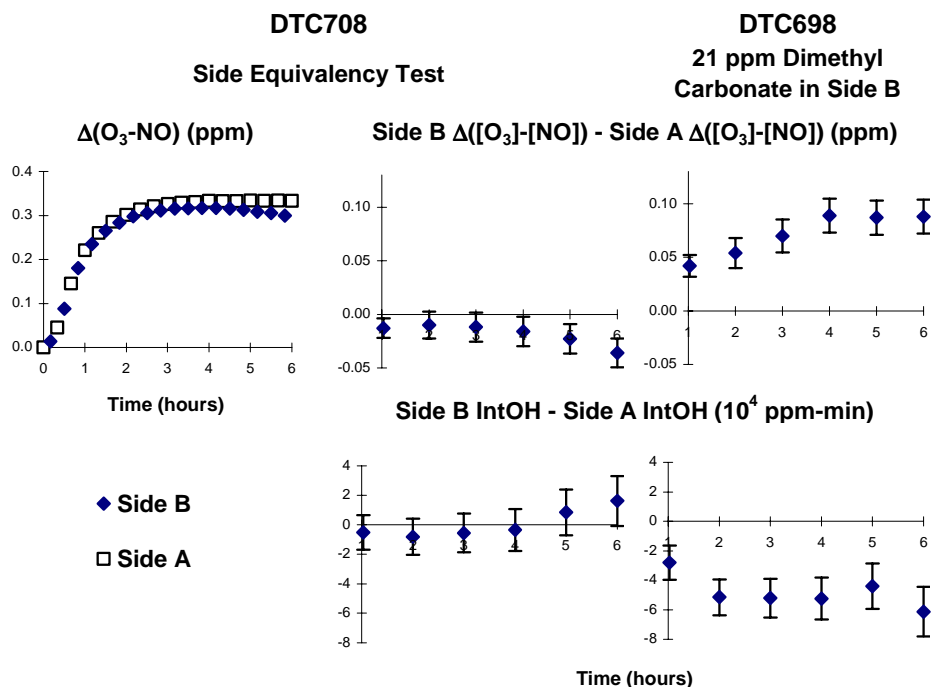


Figure 2. Selected results of the low NO_x mini-surrogate side equivalency test experiment, and comparison with comparable data obtained in the low NO_x mini-surrogate experiments with added dimethyl carbonate.

A potentially more serious problem was a lack of side equivalency observed in the side equivalency test experiment DTC709 carried out around after the last run with dimethyl carbonate. In this experiment, the same low NO_x mini-surrogate mixture was irradiated on both sides of the chamber. As indicated in Table 4, somewhat less O_3 was observed on Side B than Side A, and also the O_3 decayed more rapidly on that side once the O_3 maximum was reached. The $\Delta([\text{O}_3]\text{-}[\text{NO}])$ data and the $\Delta([\text{O}_3]\text{-}[\text{NO}])$ differences between the two sides for that experiment are shown on Figure 2. To show the bias this might introduce on the experimentally $\Delta([\text{O}_3]\text{-}[\text{NO}])$ incremental reactivities, the $\Delta([\text{O}_3]\text{-}[\text{NO}])$ differences between the two sides are also shown for the run DTC698, the low NO_x full surrogate run where dimethyl carbonate was added. It can be seen that the $\Delta([\text{O}_3]\text{-}[\text{NO}])$ reactivity bias introduced is relatively small and in the opposite direction of the effect of the dimethyl carbonate addition in run DTC698. Figure 2 also shows the side differences in the IntOH data derived from the m-xylene consumption rate measurements in those experiments. In this case the side differences are within the experimental uncertainty ranges of the measurements, and again they are small compared to the effect of adding the dimethyl carbonate.

Dimethyl Carbonate Reactivity Experiments

Five incremental reactivity experiments were carried out with dimethyl carbonate, two for each with the mini-surrogate and high NO_x full surrogate and one with the low NO_x full surrogate. The results are summarized on Table 5 and concentration-time plots of the major reactivity results are shown on Figure 3. Results of model calculations are also shown in the figure.

The results show that the incremental reactivities of dimethyl carbonate are low, with relatively large amounts of the compound being added in the experiments to obtain measurable effects. This is attributed to the relatively low rate at which this compound reacts with OH radicals. The results indicate that dimethyl carbonate has positive effects on NO oxidation and O₃ formation under most conditions. The effects of dimethyl carbonate on OH radical levels in the higher NO_x experiments is relatively low but slightly negative, but the inhibition of OH radicals is greater in the lower NO_x experiments. Note that radical inhibition in low NO_x conditions is observed for compounds can be attributed in part to effects of the VOC on NO oxidation and O₃ formation rates. Compounds such as CO that do not have radical sinks in their mechanism also inhibit IntOH in the low NO_x experiments (Carter et al, 1995b). Thus, these results indicate that dimethyl carbonate does not have significant radical sinks (or sources) in its

Table 5. Summary of conditions and selected results of the environmental chamber reactivity experiments with dimethyl carbonate and methyl isopropyl carbonate.

Run	Test VOC (ppm)	NO _x (ppm)	Surg. (ppm C)	Δ([O ₃]-[NO]) (ppm)						5 th Hour IntOH (10 ⁻⁶ min)		
				2 nd Hour			6 th Hour			Base	Test	IR [a]
				Base	Test	IR [a]	Base	Test	IR [a]			
<u>Mini-Surrogate + Dimethyl Carbonate</u>												
DTC692B	23.7	0.44	6.12	0.13	0.18	2.3e-3	0.64	0.77	5.5e-3	12.1	10.3	-0.08
DTC703B	41.2	0.42	5.71	0.10	0.18	1.8e-3	0.57	0.79	5.2e-3	11.1	9.2	-0.05
<u>High NO_x Full Surrogate + Dimethyl Carbonate</u>												
DTC693A	21.0	0.31	4.39	0.29	0.46	8.3e-3	0.60	0.86	1.2e-2	22.0	20.0	-0.09
DTC705A	15.8	0.29	4.42	0.25	0.37	7.8e-3	0.56	0.78	1.4e-2	22.1	20.5	-0.10
<u>Low NO_x Full Surrogate + Dimethyl Carbonate</u>												
DTC698B	21.4	0.10	4.18	0.30	0.36	2.5e-3	0.33	0.42	4.1e-3	17.6	13.2	-0.21
<u>Mini-Surrogate + Methyl Isopropyl Carbonate</u>												
DTC750B	4.49	0.35	5.73	0.13	0.17	0.010	0.55	0.74	0.043	12.3	9.9	-0.5
DTC759A	3.81	0.37	5.24	0.09	0.12	0.009	0.49	0.70	0.055	10.9	6.4	-1.2
<u>High NO_x Full Surrogate + Methyl Isopropyl Carbonate</u>												
DTC755A	3.08	0.29	4.29	0.26	0.50	0.079	0.55	0.88	0.108	22.4	14.7	-2.5
DTC762A	1.66	0.30	4.22	0.25	0.39	0.085	0.54	0.78	0.143	21.5	18.3	-1.9
<u>Low NO_x Full Surrogate + Methyl Isopropyl Carbonate</u>												
DTC758B	3.27	0.09	4.46	0.27	0.35	0.024	0.28	0.40	0.035	20.3	10.7	-2.9
DTC763B	1.63	0.09	4.21	0.25	0.28	0.023	0.26	0.32	0.036	19.7	13.4	-3.8

[a] IR = Incremental Reactivity = ([Test] - [Base]) / [Test Compound Added]

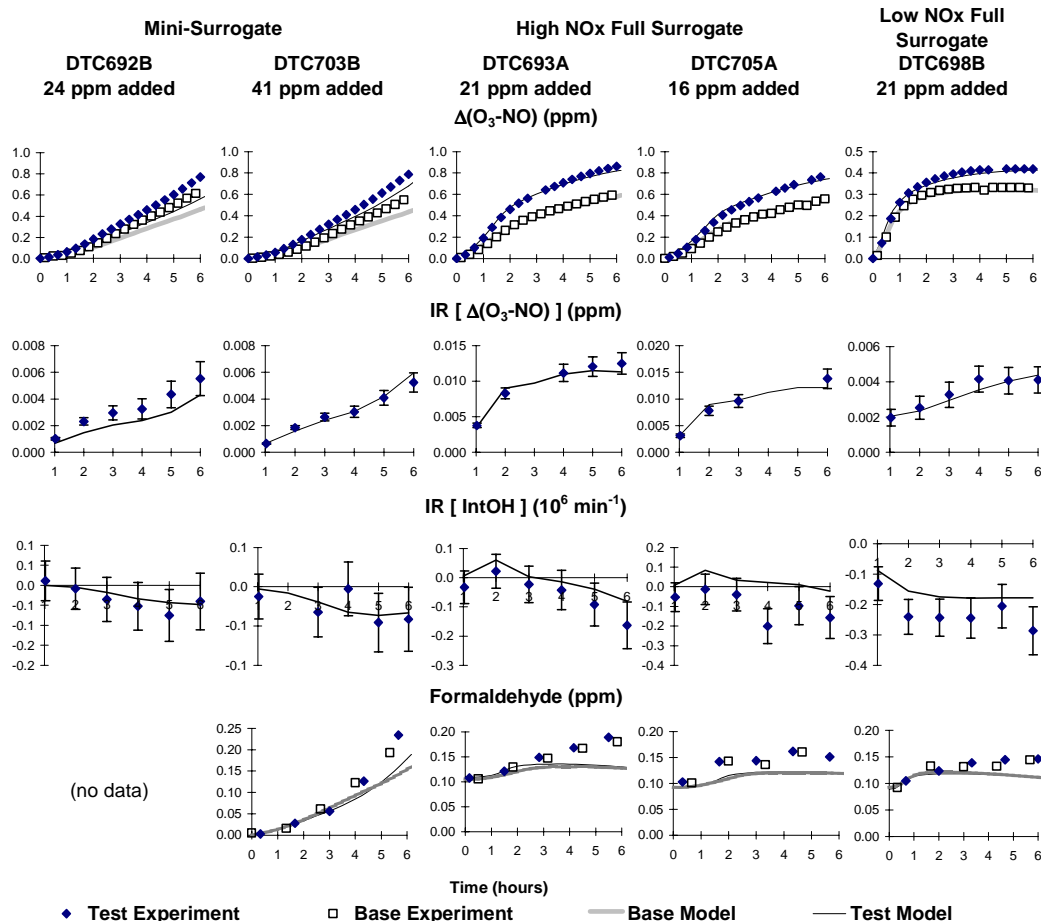


Figure 3. Selected experimental and calculated results of the incremental reactivity experiments with Dimethyl Carbonate

mechanism, and the uniformly positive effects on NO oxidation and O₃ formation is attributed to the direct NO to NO₂ conversions caused by the peroxy radicals formed when dimethyl carbonate reacts.

Consistent with the predictions of the mechanism derived for this compound, the addition of dimethyl carbonate was found not to have any effect on formaldehyde formation in the reactivity experiments. No product compounds were detected using the GC methods employed during these experiments. Note that the predicted acid and carbonate-formate products would not be detected using these methods.

Figure 3 shows that the model calculations give very good simulations of the effects of adding dimethyl carbonate in these experiments. No adjustments were made to the mechanism to achieve these fits. The slight underprediction of the IntOH inhibition in the low NO_x experiments is observed for many VOCs (including CO [Carter et al, 1995b]) and is believed to be due to problems with the base mechanism rather than necessarily being caused by problems with the test VOC.

Methyl Isopropyl Carbonate Reactivity Experiments

Six incremental reactivity experiments were carried out with dimethyl carbonate, two for each for the three types of surrogate - NO_x mixtures. The results are summarized on Table 5 and concentration-time plots of the major reactivity results are shown on Figure 4. Results of model calculations are also shown in the figure.

The incremental reactivities of methyl isopropyl carbonate are considerably higher than those for dimethyl carbonate, as would be expected due to its higher OH radical rate constant. Like dimethyl carbonate, methyl isopropyl carbonate has positive effects on NO oxidation and O₃ formation in all experiments. It has a somewhat inhibiting effect on radical levels, particularly in the full surrogate experiments. However, the inhibiting effect on radical levels is still relatively low, and is not enough to cause negative Δ([O₃]-[NO]) reactivities in the mini-surrogate experiments, which tend to be the most sensitive to effects of VOCs on radical levels.

The addition of methyl isopropyl carbonate also results in an increase in formaldehyde levels in all experiments, and also the formation of acetone, which is not formed in the reactions of any of the base surrogate components. This is consistent with the estimated mechanism for this compound.

The results of the model calculations using the estimated mechanism are also shown on Figure 4. The model gives very good fits to the effects of methyl isopropyl carbonate on NO oxidation and O₃ formation in all the experiments, and gives good simulations of the effects of this compound on formaldehyde and acetone formation. The good simulations of the acetone yields suggest that the estimates of the uncertain branching ratio for the reactions of the CH₃C(O·)(CH₃)OC(O)OCH₃ may be reasonably good. On the other hand, the model is somewhat biased towards underpredicting the inhibition of methyl isopropyl carbonate of IntOH levels, especially in the full surrogate experiments. As indicated above, an underprediction of IntOH inhibition in the low NO_x experiments is seen for many VOCs and may not be due to other problems in the mechanism besides that for the test compound (Carter et al, 1995b). On the other hand, the tendency to underpredict the IntOH inhibition in the high NO_x suggests a possible problem with the mechanism. However, given the very good fits of the model to the Δ([O₃]-[NO]) and other data in these experiments, which represent a range of chemical conditions, no attempts were made to adjust the estimated mechanism to improve these fits.

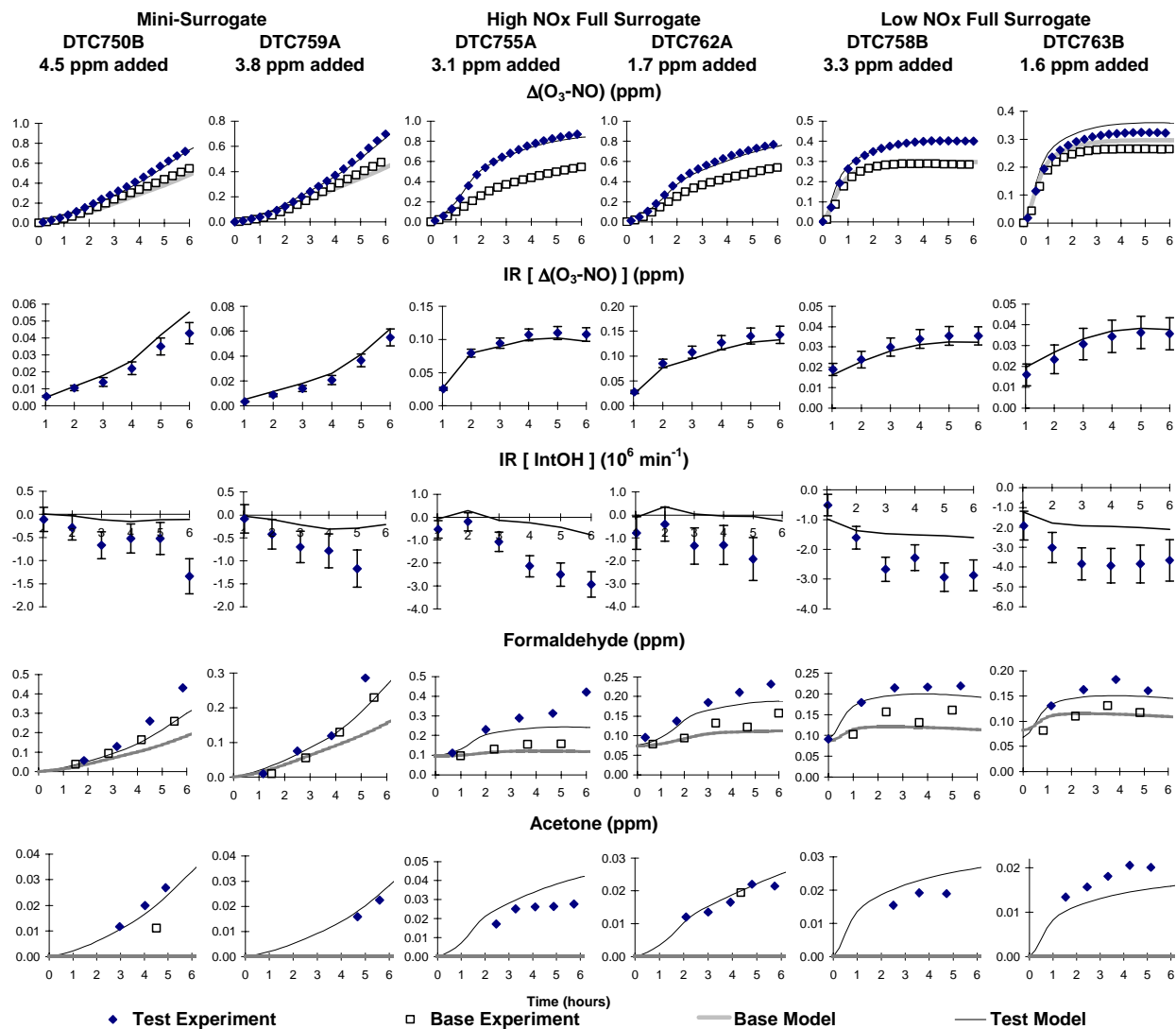


Figure 4. Selected experimental and calculated results of the incremental reactivity experiments with Methyl Isopropyl Carbonate.

ATMOSPHERIC REACTIVITY CALCULATIONS

Incremental reactivities of VOCs have been shown to be highly dependent on environmental conditions, so reactivities measured in environmental chamber experiments cannot necessarily be assumed to be the same as those under atmospheric conditions (Carter and Atkinson, 1989; Carter et al, 1995b). Because of this, the only method available to obtain quantitative estimates of incremental reactivities of VOCs in ambient air pollution episodes is to conduct airshed model simulations of the episodes. Since these simulations cannot be any more reliable than the chemical mechanisms used, the major objective of this program was to assess the reliability of the estimated dimethyl carbonate and methyl isopropyl carbonate mechanisms for use in such calculations. As discussed above, the results of the experiments indicate that the mechanisms developed in this work serve as an appropriate basis for estimating the effects of these carbonates on ozone under atmospheric conditions. The atmospheric reactivity estimates based on these mechanisms are discussed in this section. Note that the atmospheric reactivities calculated for these compounds are the same as given by Carter (2000), since the same mechanisms were employed.

Scenarios Used for Reactivity Assessment

The set of airshed scenarios employed to assess the reactivities for this study is the same as those used for calculating the MIR and other reactivity scales in our previous work (Carter, 1994a), and also in the update using the SAPRC-99 mechanism (Carter, 2000). These scenarios, and the reasons for using them, are briefly described below.

The objective is to use a set of scenarios that represents, as much as possible, a comprehensive distribution of the environmental conditions where unacceptable levels of ozone are formed. Although a set of scenarios has not been developed for the specific purpose of VOC reactivity assessment, the EPA developed an extensive set of scenarios for conducting analyses of effects of ROG and NO_x controls on ozone formation using the EKMA modeling approach (Gipson et al. 1981; Gipson and Freas, 1983; EPA, 1984; Gery et al. 1987; Baugues, 1990). The EKMA approach involves the use of single-cell box models to simulate how the ozone formation in one day episodes is affected by changes in ROG and NO_x inputs. Although single-cell models cannot represent realistic pollution episodes in great detail, they can represent dynamic injection of pollutants, time-varying changes of inversion heights, entrainment of pollutants from aloft as the inversion height rises, and time-varying photolysis rates, temperatures, and humidities (Gipson and Freas, 1981; EPA, 1984; Gipson, 1984; Hogo and Gery, 1988). Thus, they can be used to simulate a wide range of the chemical conditions which affect ozone formation from ROG and NO_x, and which affect VOC reactivity. Therefore, at least to the extent they are suitable for their intended purpose, an appropriate set of EKMA scenarios should also be suitable for assessing reactivities over a wide range of conditions.

Base Case Scenarios

The set of EKMA scenarios used in this study were developed by the United States EPA for assessing how various ROG and NO_x control strategies would affect ozone nonattainment in various areas of the country (Baugues, 1990). The characteristics of these scenarios and the methods used to derive their input data are described in more detail elsewhere (Baugues, 1990; Carter, 1994b). Briefly, 39 urban areas in the United States were selected based on geographical representativeness of ozone nonattainment areas and data availability, and a representative high ozone episode was selected for each. The initial non-methane organic carbon (NMOC) and NO_x concentrations, the aloft O₃ concentrations, and the mixing height inputs were based on measurement data for the various areas, the hourly emissions in the scenarios were obtained from the National Acid Precipitation Assessment Program emissions inventory (Baugues, 1990), and biogenic emissions were also included. Table 6 gives a summary of the urban areas represented and other selected characteristics of the scenarios.

Several changes to the scenario inputs were made based on discussions with the California ARB staff and others (Carter, 1994a,b). Two percent of the initial NO_x and 0.1% of the emitted NO_x in all the scenarios was assumed to be in the form of HONO. The photolysis rates were calculated using solar light intensities and spectra calculated by Jeffries (1991) for 640 meters, the approximate mid-point of the mixed layer during daylight hours. The composition of the non methane organic pollutants entrained from aloft was based on the analysis of Jeffries et al. (1989). The composition of the initial and emitted reactive organics was derived as discussed below. Complete listings of the input data for the scenarios are given elsewhere (Carter, 1994b).

This set of 39 EKMA scenarios are referred to as “base case” to distinguish them from the scenarios derived from them by adjusting NO_x inputs to yield standard conditions of NO_x availability as discussed below. No claim is made as to the accuracy of these scenarios in representing any real episode, but they are a result of an effort to represent, as accurately as possible given the available data and the limitations of the formulation of the EKMA model, the range of conditions occurring in urban areas throughout the United States. When developing general reactivity scales it is more important that the scenarios employed represent a realistic distribution of chemical conditions than accurately representing the details of any one particular episode.

The Base ROG mixture is the mixture of reactive organic gases used to represent the chemical composition of the initial and emitted anthropogenic reactive organic gases from all sources in the scenarios. Consistent with the approach used in the original EPA scenarios, the same mixture was used for all scenarios. The speciation for this mixture was derived by Croes (1991) based on an analysis of the EPA database (Jeffries et al. 1989) for the hydrocarbons and the 1987 Southern California Air Quality Study (SCAQS) database for the oxygenates (Croes et al. 1994; Lurmann and Main. 1992). This mixture consists of 52% (by carbon) alkanes, 15% alkenes, 27% aromatics, 1% formaldehyde, 2% higher aldehydes, 1% ketones, and 2% acetylene. The detailed composition of this mixture is given elsewhere (Carter, 1994b; Carter, 2000).

Table 6. Summary of the conditions of the scenarios used for atmospheric reactivity assessment.

Scenario		Max O ₃ (ppb)	Max 8- Hr Avg O ₃ (ppb)	ROG / NO _x	NO _x / MOIR NO _x	Height (kM)	Init., Emit ROG (m. mol m ⁻²)	O ₃ aloft (ppb)	Integrated OH (ppt-min)
Avg.	MIR	187	119	3.1	1.5	1.8	15	70	128
Cond.	MOIR	239	165	4.5	1.0	1.8	15	70	209
	EBIR	227	172	6.4	0.7	1.8	15	70	210
Base	Atlanta, GA	179	132	7.3	0.7	2.1	12	63	200
Case	Austin, TX	175	144	9.3	0.5	2.1	11	85	179
	Baltimore, MD	334	215	5.2	1.1	1.2	17	84	186
	Baton Rouge, LA	241	173	6.8	0.9	1.0	11	62	186
	Birmingham, AL	244	202	6.9	0.5	1.8	13	81	208
	Boston, MA	197	167	6.5	0.6	2.6	14	105	262
	Charlotte, NC	143	126	7.8	0.3	3.0	7	92	212
	Chicago, IL	278	226	11.6	0.5	1.4	25	40	164
	Cincinnati, OH	205	153	6.4	0.7	2.8	17	70	220
	Cleveland, OH	252	179	6.6	0.9	1.7	16	89	187
	Dallas, TX	208	141	4.7	1.2	2.3	18	75	176
	Denver, CO	204	139	6.3	1.1	3.4	29	57	143
	Detroit, MI	246	177	6.8	0.7	1.8	17	68	235
	El Paso, TX	182	135	6.6	1.0	2.0	12	65	138
	Hartford, CT	172	144	8.4	0.5	2.3	11	78	220
	Houston, TX	312	217	6.1	0.9	1.7	25	65	225
	Indianapolis, IN	212	148	6.6	0.9	1.7	12	52	211
	Jacksonville, FL	155	115	7.6	0.6	1.5	8	40	206
	Kansas City, MO	159	126	7.1	0.6	2.2	9	65	233
	Lake Charles, LA	286	209	7.4	0.6	0.5	7	40	233
	Los Angeles, CA	568	406	7.6	1.0	0.5	23	100	134
	Louisville, KY	212	155	5.5	0.8	2.5	14	75	260
	Memphis, TN	229	180	6.8	0.6	1.8	15	58	249
	Miami, FL	132	111	9.6	0.4	2.7	9	57	181
	Nashville, TN	167	138	8.0	0.4	1.6	7	50	225
	New York, NY	365	294	8.1	0.7	1.5	39	103	159
	Philadelphia, PA	247	169	6.2	0.9	1.8	19	53	227
	Phoenix, AZ	277	193	7.6	1.0	3.3	40	60	153
	Portland, OR	166	126	6.5	0.7	1.6	6	66	233
	Richmond, VA	242	172	6.2	0.8	1.9	16	64	217
	Sacramento, CA	204	142	6.6	0.8	1.1	7	60	209
	St Louis, MO	324	209	6.1	1.1	1.6	26	82	176
	Salt Lake City, UT	186	150	8.5	0.6	2.2	11	85	182
	San Antonio, TX	133	98	3.9	1.0	2.3	6	60	192
San Diego, CA	193	150	7.1	0.9	0.9	8	90	146	
San Francisco, CA	229	126	4.8	1.8	0.7	25	70	61	
Tampa, FL	230	153	4.4	1.0	1.0	8	68	211	
Tulsa, OK	231	160	5.3	0.9	1.8	15	70	264	
Washington, DC	283	209	5.3	0.8	1.4	13	99	239	

Adjusted NO_x scenarios

Incremental reactivities in the base case scenarios would be expected to vary widely, since incremental reactivities depend on the ROG/NO_x ratio, and that ratio varies widely among the base case scenarios. To obtain reactivity scales for specified NO_x conditions, separate scenarios, designated MIR (for maximum incremental reactivity), MOIR (for maximum ozone incremental reactivity), and Equal Benefit Incremental Reactivity (EBIR) were developed (Carter, 1994a). In the MIR scenarios, the NO_x inputs were adjusted so the base ROG mixture (and most other VOCs) has its highest incremental reactivity. This is representative of the highest NO_x conditions of relevance to VOC reactivity assessment because at higher NO_x levels O₃ yields become significantly suppressed, but is also the condition where O₃ is most sensitive to VOC emissions. In the MOIR scenarios, the NO_x inputs were adjusted to yield the highest ozone concentration. In the EBIR scenarios, the NO_x inputs were adjusted so that the relative effects of NO_x reductions and total ROG reductions on peak ozone levels were equal. This represents the lowest NO_x condition of relevance for VOC reactivity assessment, because O₃ formation becomes more sensitive to NO_x emissions than VOC emissions at lower NO_x levels. As discussed by Carter (1994a) the MIR and EBIR ROG/NO_x ratios are respectively ~1.5 and ~0.7 times those for the MOIR scenarios in all cases.

NO_x Conditions in the Base Case Scenarios

The variability of ROG/NO_x ratios in the base case scenarios suggests a variability of reactivity characteristics in those scenarios. However, as discussed previously (Carter, 1994a), the ROG/NO_x ratio is also variable in the MIR or MOIR scenarios, despite the fact that the NO_x inputs in these scenarios are adjusted to yield a specified reactivity characteristic. Thus, the ROG/NO_x ratio, by itself, is not necessarily a good predictor of reactivity characteristics of a particular scenario. The NO_x/NO_x^{MOIR} ratio is a much better predictor of this, with values greater than 1 indicating relatively high NO_x conditions where ozone formation is more sensitive to VOCs, and values less than 1 indicating NO_x-limited conditions. NO_x/NO_x^{MOIR} ratios less than 0.7 represent conditions where NO_x control is a more effective ozone control strategy than ROG control (Carter, 1994a). Note that more than half of the base case scenarios represent NO_x-limited conditions, and ~25% of them represent conditions where NO_x control is more beneficial than VOC control. A relatively small number of scenarios represent MIR or near MIR conditions. However, as discussed elsewhere (Carter, 1994a), this set of scenarios is based on near-worst-case conditions for ozone formation in each of the airsheds. Had scenarios representing less-than-worst-case conditions been included, one might expect a larger number of MIR or near MIR scenarios. This is because NO_x is consumed more slowly on days with lower light intensity or temperature, and thus the scenario is less likely to become NO_x-limited.

Quantification of Atmospheric Reactivity

The reactivity of a VOC in an airshed scenario is measured by its incremental reactivity. For ambient scenarios, this is defined as the change in ozone caused by adding the VOC to the emissions,

divided by the amount of VOC added, calculated for sufficiently small amounts of added VOC that the incremental reactivity is independent of the amount added³.

$$\text{IR}(\text{VOC}, \text{Scenario}) = \lim_{\text{VOC} \rightarrow 0} \left[\frac{\text{O}_3(\text{Scenario with VOC}) - \text{O}_3(\text{Base Scenario})}{\text{Amount of VOC Added}} \right] \quad (\text{V})$$

The specific calculation procedure is discussed in detail elsewhere (Carter, 1994a,b).

Incremental reactivities derived as given above tend to vary from scenario to scenario because they differ in their overall sensitivity of O₃ formation to VOCs. These differences can be factored out to some extent by using “relative reactivities”, which are defined as ratios of incremental reactivities to the incremental reactivity of the base ROG mixture, which is used to represent emissions of reactive VOCs from all sources.

$$\text{RR}(\text{VOC}, \text{Scenario}) = \frac{\text{IR}(\text{VOC}, \text{Scenario})}{\text{IR}(\text{Base ROG}, \text{Scenario})} \quad (\text{VI})$$

These relative reactivities can also be thought of as the relative effect on O₃ of controlling emissions of the particular VOC by itself, compared to controlling emissions from all VOC sources equally. Thus, they are more meaningful in terms of control strategy assessment than absolute reactivities, which can vary greatly depending on the episode and local meteorology.

In addition to depending on the VOC and the scenario, the incremental and relative reactivities depend on how the amounts of VOC added are quantified. In this work, this is quantified on a mass basis, since this is how VOCs are regulated, and generally approximates how VOC substitutions are made in practice. Note that relative reactivities will be different if they are quantified on a molar basis, with VOCs with higher molecular weight having higher reactivities on a mole basis than a gram basis.

Relative reactivities can also depend significantly on how ozone impacts are quantified (Carter, 1994a). Two different ozone quantification methods are used in this work, as follows:

“Ozone Yield” reactivities measure the effect of the VOC on the total amount of ozone formed in the scenario at the time of its maximum concentration. Incremental reactivities are quantified as grams O₃ formed per gram VOC added. Most previous recent studies of ozone reactivity (Dodge, 1984; Carter and Atkinson, 1987, 1989, Chang and Rudy, 1990; Jeffries and Crouse, 1991) have been based on this quantification method. The MIR, MOIR, and EBIR scales of Carter (1994a) also use this quantification.

“Maximum 8 Hour Average” reactivities measure the effect of the VOC on the average ozone concentration during the 8-hour period when the average ozone concentration was the greatest, which in

³ Note that this differs from how the term “incremental reactivity” is used in the context of chamber experiments. In that case, the incremental reactivity refers to the relative change observed in the individual experiments, which in general depends on the amount added.

these one-day scenarios was the last 8 hours of the simulation. This provides a measure of ozone impact that is more closely related to the new Federal ozone standard that is given in terms of an 8 hour average. This quantification is used for relative reactivities in this work.

In previous reports, we have reported reactivities in terms of integrated O₃ over a standard concentration of 0.09 or 0.12 ppm. This provides a measure of the effect of the VOC on exposure to unacceptable levels of ozone. This is replaced by the maximum 8 hour average reactivities because it is more representative of the proposed new Federal ozone standard and because reactivities relative to integrated O₃ over a standard tend to be between those relative to ozone yield and those relative to 8-hour averages. Therefore, presenting both ozone yield and maximum 8-hour average relative reactivities should be sufficient to provide information on how relative reactivities vary with ozone quantification method. Incremental reactivities are quantified as ppm O₃ per milligram VOC emitted per square meter, but maximum 8 hour average reactivities are usually quantified as relative reactivities quantified on a mass basis.

Note that incremental reactivities are calculated for a total of 156 scenarios, consisting of the 39 base case scenarios and the three adjusted NO_x scenarios for each of the 39 base case scenarios. However, the incremental reactivities in the MIR, MOIR, or EBIR) scales are reported as averages of the incremental reactivities in the corresponding adjusted NO_x scenarios, because adjusting the NO_x conditions reduces the scenario variability, and this allows for a derivation single reactivity scales representing each type of NO_x condition. On the other hand, the individual scenario results will be shown for the base case scenarios, to give an indication of the scenario-to-scenario variability of the calculated reactivity results.

Results

Table 7 lists the ozone yield incremental reactivities calculated for dimethyl carbonate, methyl isopropyl carbonate, ethane, propane and the mixture of emitted reactive organic compounds (the base ROG). Table 8 gives the ozone yield and maximum 8-hour average reactivities relative to the base ROG for these compounds. Ethane is chosen for comparison because it has been used by the EPA as the informal standard to determine “negligible” reactivity for VOC exemption purposes (Dimitriades, 1999). If a compound does not have a significantly greater impact on ozone than ethane in most or all the scenarios, it might be reasonably be considered for exemption from regulation as an ozone precursor. Propane is shown for comparison with methyl isopropyl carbonate, which as can be seen from the tables has comparable reactivity.

The results show that dimethyl carbonate has an extremely low impact on O₃ formation, with the O₃ impact on a mass basis being less than 4% that of the mixture used to represent reactive VOC emissions from all sources. The relative impact is about the same regardless of whether the reactivities are relative to the peak O₃ or the maximum 8-hour averages, though the impact relative to the base ROG tend to be lower in the higher NO_x scenarios, which is also the case for ethane. This is because the higher NO_x

Table 7. Atmospheric incremental reactivities calculated for the base ROG mixture, ethane, dimethyl carbonate (DMC), methyl isopropyl carbonate (MIPR-CB) and propane.

Scenario	Incremental Reactivities (gm O ₃ / gm VOC)				
	Base ROG	Ethane	DMC	MIPR-CB	Propane
Adj'd MIR	3.68	0.30	0.058	0.69	0.56
NOx MOIR	1.46	0.20	0.042	0.39	0.36
EBIR	0.85	0.15	0.034	0.28	0.26
Base Average	1.03	0.15	0.035	0.30	0.27
Case St.Dev	0.42	0.04	0.007	0.07	0.07
ATL GA	0.82	0.13	0.031	0.27	0.23
AUS TX	0.63	0.12	0.029	0.23	0.21
BAL MD	1.59	0.20	0.043	0.40	0.36
BAT LA	0.85	0.11	0.030	0.27	0.21
BIR AL	0.72	0.16	0.033	0.26	0.27
BOS MA	0.72	0.14	0.034	0.26	0.26
CHA NC	0.53	0.11	0.027	0.20	0.19
CHI IL	0.26	0.07	0.021	0.16	0.13
CIN OH	1.12	0.20	0.040	0.33	0.35
CLE OH	1.17	0.15	0.037	0.34	0.29
DAL TX	2.14	0.23	0.044	0.48	0.40
DEN CO	1.66	0.15	0.038	0.40	0.29
DET MI	0.98	0.18	0.037	0.30	0.31
ELP TX	1.45	0.14	0.032	0.35	0.26
HAR CT	0.77	0.16	0.034	0.25	0.27
HOU TX	1.10	0.17	0.038	0.33	0.31
IND IN	1.24	0.18	0.041	0.35	0.32
JAC FL	0.67	0.11	0.031	0.25	0.20
KAN MO	1.07	0.20	0.040	0.32	0.35
LAK LA	0.42	0.09	0.030	0.22	0.18
LOS CA	0.76	0.08	0.023	0.22	0.16
LOU KY	1.24	0.22	0.045	0.38	0.38
MEM TN	0.76	0.15	0.036	0.27	0.26
MIA FL	0.49	0.10	0.026	0.20	0.16
NAS TN	0.67	0.15	0.033	0.25	0.25
NEW NY	0.39	0.07	0.028	0.20	0.16
PHI PA	1.08	0.17	0.039	0.32	0.30
PHO AZ	1.46	0.18	0.034	0.35	0.31
POR OR	0.96	0.17	0.037	0.30	0.29
RIC VA	1.06	0.18	0.040	0.32	0.32
SAC CA	1.22	0.19	0.035	0.33	0.31
SAI MO	1.38	0.16	0.037	0.35	0.30
SAL UT	0.90	0.15	0.031	0.27	0.26
SAN TX	1.62	0.21	0.039	0.40	0.36
SDO CA	0.85	0.09	0.028	0.25	0.19
SFO CA	1.87	0.09	0.019	0.27	0.18
TAM FL	1.52	0.19	0.046	0.42	0.35
TUL OK	1.17	0.20	0.046	0.37	0.36
WAS DC	0.99	0.18	0.039	0.31	0.32

Table 8. Atmospheric relative reactivities calculated for ethane, dimethyl carbonate (DMC), methyl isopropyl carbonate (MIPR-CB) and propane.

Scenario		Reactivities relative to the base ROG (mass basis)							
		Ozone Yield				Max 8 Hour Average			
		Ethane	DMC	MIPR-CB	Propane	Ethane	DMC	MIPR-CB	Propane
Adj'd	MIR	0.08	0.016	0.19	0.15	0.07	0.015	0.17	0.13
NO _x	MOIR	0.13	0.029	0.27	0.24	0.08	0.021	0.21	0.17
	EBIR	0.17	0.041	0.33	0.31	0.10	0.027	0.25	0.19
Base	Average	0.16	0.038	0.32	0.29	0.10	0.027	0.24	0.19
Case	St.Dev	0.04	0.014	0.08	0.08	0.02	0.008	0.05	0.04
	ATL GA	0.16	0.038	0.33	0.28	0.09	0.028	0.26	0.19
	AUS TX	0.19	0.046	0.37	0.33	0.11	0.036	0.30	0.23
	BAL MD	0.12	0.027	0.25	0.23	0.08	0.018	0.19	0.15
	BAT LA	0.13	0.036	0.32	0.25	0.08	0.026	0.25	0.18
	BIR AL	0.22	0.046	0.36	0.38	0.12	0.031	0.27	0.23
	BOS MA	0.20	0.047	0.36	0.35	0.13	0.035	0.29	0.25
	CHA NC	0.21	0.051	0.38	0.37	0.14	0.042	0.34	0.27
	CHI IL	0.28	0.081	0.60	0.51	0.13	0.045	0.36	0.27
	CIN OH	0.18	0.036	0.30	0.31	0.10	0.025	0.22	0.19
	CLE OH	0.13	0.031	0.29	0.24	0.08	0.021	0.21	0.16
	DAL TX	0.11	0.021	0.22	0.18	0.08	0.018	0.20	0.15
	DEN CO	0.09	0.023	0.24	0.18	0.06	0.017	0.19	0.13
	DET MI	0.18	0.038	0.31	0.32	0.10	0.025	0.23	0.19
	ELP TX	0.10	0.022	0.24	0.18	0.07	0.018	0.20	0.13
	HAR CT	0.20	0.044	0.33	0.34	0.12	0.033	0.28	0.23
	HOU TX	0.16	0.035	0.30	0.28	0.09	0.024	0.22	0.18
	IND IN	0.14	0.033	0.28	0.26	0.09	0.023	0.22	0.17
	JAC FL	0.16	0.046	0.37	0.29	0.09	0.031	0.27	0.19
	KAN MO	0.19	0.038	0.30	0.33	0.11	0.028	0.24	0.21
	LAK LA	0.22	0.071	0.51	0.42	0.11	0.043	0.34	0.25
	LOS CA	0.11	0.030	0.28	0.21	0.07	0.020	0.20	0.14
	LOU KY	0.17	0.037	0.31	0.30	0.11	0.028	0.25	0.21
	MEM TN	0.20	0.047	0.36	0.35	0.11	0.031	0.27	0.21
	MIA FL	0.20	0.053	0.41	0.33	0.11	0.039	0.32	0.22
	NAS TN	0.23	0.049	0.37	0.38	0.15	0.040	0.32	0.27
	NEW NY	0.17	0.071	0.51	0.41	0.08	0.032	0.27	0.20
	PHI PA	0.16	0.036	0.30	0.28	0.09	0.025	0.23	0.18
	PHO AZ	0.12	0.023	0.24	0.21	0.08	0.017	0.18	0.14
	POR OR	0.17	0.038	0.32	0.30	0.11	0.030	0.27	0.21
	RIC VA	0.17	0.037	0.30	0.31	0.09	0.024	0.22	0.18
	SAC CA	0.15	0.029	0.27	0.26	0.09	0.021	0.21	0.17
	SAI MO	0.11	0.027	0.25	0.22	0.07	0.019	0.19	0.15
	SAL UT	0.17	0.035	0.30	0.29	0.10	0.024	0.23	0.18
	SAN TX	0.13	0.024	0.25	0.22	0.09	0.021	0.21	0.17
	SDO CA	0.11	0.033	0.29	0.22	0.08	0.024	0.23	0.16
	SFO CA	0.05	0.010	0.15	0.10	0.04	0.010	0.14	0.09
	TAM FL	0.12	0.030	0.28	0.23	0.08	0.022	0.22	0.17
	TUL OK	0.17	0.039	0.31	0.30	0.10	0.025	0.23	0.19
	WAS DC	0.18	0.039	0.32	0.32	0.10	0.026	0.23	0.20

levels suppress radicals, and thus the relative amounts of the slower reacting compounds that react in the scenario. The reactivity of dimethyl carbonate is about 20-25% that of ethane on a mass basis (or about 60-70% on a molar basis), with the reactivity relative to ethane not being strongly dependent on scenario conditions or how ozone impacts are quantified.

Methyl isopropyl carbonate is much more reactive than dimethyl carbonate, but is still a relatively low reactivity compound. Its effect on ozone formation is about 1/5 - 1/3 that of the base ROG mixture on a mass basis. Its relative reactivity tends to be slightly higher in terms of effect on peak ozone concentrations than in terms of effects on maximum 8-hour averages, and its relative reactivities also tend to be higher in the lower NO_x scenarios. As shown on the tables, its ozone impacts are comparable to that of propane.

CONCLUSIONS

The decision whether it is appropriate to regulate a compound as an ozone precursor requires a quantitative assessment of its ozone impacts under a variety of environmental conditions. This involves developing a chemical mechanism for the compound's atmospheric reactions that can be reliably used in airshed models to predict its atmospheric reactivity. Until this study, there was no experimental information concerning the impacts of dimethyl carbonate and methyl isopropyl carbonate on ozone formation, and thus reactivity estimates for these compounds were highly uncertain. The objective of this study was to develop mechanisms for the atmospheric reactions of these compounds that can accurately predict the ozone impacts of this compound under a variety of simulated atmospheric conditions, and then use them to estimate their atmospheric ozone impacts. We believe this program was successful in achieving this objective.

The atmospheric reaction mechanisms developed for the carbonates studied in this work were found to give sufficiently good simulations of the effects of these compounds on NO oxidation, O₃ formation and other manifestations of reactivity that they should serve as a reliable basis for estimating their ozone impacts in the atmosphere. These mechanisms employed measured rate constants for the reactions of these compounds with OH radicals, and estimates for the subsequent reactions of the radicals formed using the mechanism estimation procedure associated with the SAPRC-99 mechanism (Carter, 2000). The mechanism for dimethyl carbonate was fairly straightforward, with the only uncertainty being a branching ratio that only affects relative yields of very low reactivity products, and has no effect on predictions of atmospheric ozone impact. The mechanism for methyl isopropyl carbonate was more complex, and had several uncertainties that might affect ozone impact predictions. However, no adjustments had to be made to the mechanism to obtain satisfactory results when simulating environmental chamber experiments with this compound. This suggests that the estimation procedures associated with the SAPRC-99 may perform reasonably well for this type of compound.

Based on the mechanism developed for this work, the ozone impact for dimethyl carbonate was calculated to be very low. It was calculated to be no more than ~4% of the ozone as an equal mass of the mixture representing VOC emissions from all sources, and no more than about 30% that of an equal mass of ethane. Its ozone impact was lower than that of ethane even when computed on a molar basis. Therefore, if ethane is used as the standard for defining negligible" reactivity for VOC exemption purposes, then this compound could appropriately be exempted on this basis.

On the other hand, the mass-based ozone impact of methyl isopropyl carbonate is calculated to be approximately twice that of ethane under most conditions, so exempting this compound may not be appropriate under that standard. However, methyl isopropyl carbonate still has a relatively low ozone impact, being between 1/5 and 1/3 that of an equal mass the mixture representing VOC emissions from all sources, and being comparable to that of propane. This means that regulation of emissions of this compound is about 3-5 times less effective in reducing ozone as regulation of all VOC sources equally.

REFERENCES

- Atkinson, R. (1989): "Kinetics and Mechanisms of the Gas-Phase Reactions of the Hydroxyl Radical with Organic Compounds," J. Phys. Chem. Ref. Data, Monograph no 1.
- Atkinson, R. (1991): "Kinetics and Mechanisms of the Gas-Phase Reactions of the NO₃ Radical with Organic Compounds," J. Phys. Chem. Ref. Data, 20, 459-507.
- Atkinson, R. (1994): "Gas-Phase Tropospheric Chemistry of Organic Compounds," J. Phys. Chem. Ref. Data, Monograph No. 2.
- Atkinson, R. (1997): "Gas Phase Tropospheric Chemistry of Volatile Organic Compounds: 1. Alkanes and Alkenes," J. Phys. Chem. Ref. Data, 26, 215-290.
- Atkinson, R., S. M. Aschmann (1985): "Kinetics of the Gas Phase Reaction of Cl Atoms with a Series of Organics at 296 ± 2 K and Atmospheric Pressure," Int. J. Chem. Kinet. 17, 33.
- Atkinson, R. and W. P. L. Carter (1984): "Kinetics and Mechanisms of the Gas-Phase Reactions of Ozone with Organic Compounds under Atmospheric Conditions," Chem. Rev. 84, 437-470.
- Baugues, K. (1990): "Preliminary Planning Information for Updating the Ozone Regulatory Impact Analysis Version of EKMA," Draft Document, Source Receptor Analysis Branch, Technical Support Division, U. S. Environmental Protection Agency, Research Triangle Park, NC, January.
- Becker, K. H. and C. G. Sauer (2000): "Atmospheric Degradation of C3 Formaldehyde Acetals," Report, Ber. - Bergische Univ., Gesamthochsch. Wuppertal, Fachbereich 9, Phys. Chem. From abstract on CAS database.
- Bilde, M., T. E. Mgelberg, J. Sehested, O. J. Nielsen, T. J. Wallington, M. D. Hurley, S. M. Japar, M. Dill, V. L. Orkin, T. J. Buckley, R. E. Huie, and M. J. Kurylo (1997), "Atmospheric Chemistry of Dimethyl Carbonate: Reaction with OH Radicals, UV Spectra of CH₃OC(O)OCH₂ and CH₃OC(O)OCH₂O₂ Radicals, Reactions of CH₃OC(O)OCH₂O₂ with NO and NO₂, and Fate of CH₃OC(O)OCH₂O₂ Radicals," J. Phys. Chem. A, 3514-3525.
- CARB (1999) California Air Resources Board, Proposed Regulation for Title 17, California Code of Regulations, Division 3, Chapter 1, Subchapter 8.5, Article 3.1, sections 94560- 94539.
- Carter, W. P. L. (1990): "A Detailed Mechanism for the Gas-Phase Atmospheric Reactions of Organic Compounds," Atmos. Environ., 24A, 481-518.
- Carter, W. P. L. (1994a): "Development of Ozone Reactivity Scales for Volatile Organic Compounds," J. Air & Waste Manage. Assoc., 44, 881-899.
- Carter, W. P. L. (1994b): "Calculation of Reactivity Scales Using an Updated Carbon Bond IV Mechanism," Report Prepared for Systems Applications International Under Funding from the Auto/Oil Air Quality Improvement Research Program, April 12. Available at <http://helium.ucr.edu/~carter/absts.htm#cb4rct>.

- Carter, W. P. L. (2000): "Documentation of the SAPRC-99 Chemical Mechanism for VOC Reactivity Assessment," Report to the California Air Resources Board, Contracts 92-329 and 95-308, May 8. Available at <http://helium.ucr.edu/~carter/absts.htm#saprc99>.
- Carter, W. P. L. and R. Atkinson (1987): "An Experimental Study of Incremental Hydrocarbon Reactivity," *Environ. Sci. Technol.*, 21, 670-679
- Carter, W. P. L. and R. Atkinson (1989): "A Computer Modeling Study of Incremental Hydrocarbon Reactivity", *Environ. Sci. Technol.*, 23, 864.
- Carter, W. P. L., and F. W. Lurmann (1990): "Evaluation of the RADM Gas-Phase Chemical Mechanism," Final Report, EPA-600/3-90-001.
- Carter, W. P. L. and F. W. Lurmann (1991): "Evaluation of a Detailed Gas-Phase Atmospheric Reaction Mechanism using Environmental Chamber Data," *Atm. Environ.* 25A, 2771-2806.
- Carter, W. P. L., J. A. Pierce, I. L. Malkina, D. Luo and W. D. Long (1993): "Environmental Chamber Studies of Maximum Incremental Reactivities of Volatile Organic Compounds," Report to Coordinating Research Council, Project No. ME-9, California Air Resources Board Contract No. A032-0692; South Coast Air Quality Management District Contract No. C91323, United States Environmental Protection Agency Cooperative Agreement No. CR-814396-01-0, University Corporation for Atmospheric Research Contract No. 59166, and Dow Corning Corporation. April 1. Available at <http://helium.ucr.edu/~carter/absts.htm#rct1rept>.
- Carter, W. P. L., J. A. Pierce, D. Luo, and I. L. Malkina (1995a): "Environmental Chamber Studies of Maximum Incremental Reactivities of Volatile Organic Compounds," *Atmos. Environ.* 29, 2499-2511.
- Carter, W. P. L., D. Luo, I. L. Malkina, and J. A. Pierce (1995b): "Environmental Chamber Studies of Atmospheric Reactivities of Volatile Organic Compounds. Effects of Varying ROG Surrogate and NO_x," Final report to Coordinating Research Council, Inc., Project ME-9, California Air Resources Board, Contract A032-0692, and South Coast Air Quality Management District, Contract C91323. March 24. Available at <http://helium.ucr.edu/~carter/absts.htm#rct2rept>.
- Carter, W. P. L., D. Luo, I. L. Malkina, and D. Fitz (1995c): "The University of California, Riverside Environmental Chamber Data Base for Evaluating Oxidant Mechanism. Indoor Chamber Experiments through 1993," Report submitted to the U. S. Environmental Protection Agency, EPA/AREAL, Research Triangle Park, NC., March 20. Available at <http://helium.ucr.edu/~carter/absts.htm#databas>.
- Carter, W. P. L., D. Luo, I. L. Malkina, and J. A. Pierce (1995d): "Environmental Chamber Studies of Atmospheric Reactivities of Volatile Organic Compounds. Effects of Varying Chamber and Light Source," Final report to National Renewable Energy Laboratory, Contract XZ-2-12075, Coordinating Research Council, Inc., Project M-9, California Air Resources Board, Contract A032-0692, and South Coast Air Quality Management District, Contract C91323, March 26. Available at <http://helium.ucr.edu/~carter/absts.htm#explrept>.
- Carter, W. P. L., D. Luo, and I. L. Malkina (1997): "Environmental Chamber Studies for Development of an Updated Photochemical Mechanism for VOC Reactivity Assessment," Final report to the California Air Resources Board, the Coordinating Research Council, and the National Renewable Energy Laboratory, November 26. Available at <http://helium.ucr.edu/~carter/absts.htm#rct3rept>.

- Carter, W. P. L., D. Luo and I. L. Malkina (2000a): "Investigation of Atmospheric Reactivities of Selected Consumer Product VOCs," Report to California Air Resources Board, May 30. Available at <http://helium.ucr.edu/~carter/absts.htm#cpreport>.
- Chang, T. Y. and S. J. Rudy (1990): "Ozone-Forming Potential of Organic Emissions from Alternative-Fueled Vehicles," *Atmos. Environ.*, 24A, 2421-2430.
- Christensen, L. K., J. C. Ball and T. J. Wallington (2000): "Atmospheric Oxidation Mechanism of Methyl Acetate," *J. Phys. Chem. A*, 104, 345-351.
- Croes, B. E., Technical Support Division, California Air Resources Board, personal communication (1991).
- Croes, B. E., *et al.* (1994): "Southern California Air Quality Study Data Archive," Research Division, California Air Resources Board.
- Dasgupta, P. K, Dong, S. and Hwang, H. (1988): "Continuous Liquid Phase Fluorometry Coupled to a Diffusion Scrubber for the Determination of Atmospheric Formaldehyde, Hydrogen Peroxide, and Sulfur Dioxide," *Atmos. Environ.* 22, 949-963.
- Dasgupta, P.K, Dong, S. and Hwang, H. (1990): *Aerosol Science and Technology* 12, 98-104
- Dimitriades, B. (1999): "Scientific Basis of an Improved EPA Policy on Control of Organic Emissions for Ambient Ozone Reduction," *J. Air & Waste Manage. Assoc.* 49, 831-838
- Dodge, M. C. (1984): "Combined effects of organic reactivity and NMHC/NO_x ratio on photochemical oxidant formation -- a modeling study," *Atmos. Environ.*, 18, 1657.
- EPA (1984): "Guideline for Using the Carbon Bond Mechanism in City-Specific EKMA," EPA-450/4-84-005, February.
- Febo, A., C. Perrino, M. Gerardi and R. Sparapini (1995): "Evaluation of a High-Purity and High Stability Continuous Generation System for Nitrous Acid," *Environ. Sci. Technol.* 29, 2390-2395.
- Gery, M. W., R. D. Edmond and G. Z. Whitten (1987): "Tropospheric Ultraviolet Radiation. Assessment of Existing Data and Effects on Ozone Formation," Final Report, EPA-600/3-87-047, October.
- Gipson, G. L., W. P. Freas, R. A. Kelly and E. L. Meyer (1981): "Guideline for Use of City-Specific EKMA in Preparing Ozone SIPs, EPA-450/4-80-027, March.
- Gipson, G. L. and W. P. Freas (1983): "Use of City-Specific EKMA in the Ozone RIA," U. S. Environmental Protection Agency, July.
- Johnson, G. M. (1983): "Factors Affecting Oxidant Formation in Sydney Air," in "The Urban Atmosphere -- Sydney, a Case Study." Eds. J. N. Carras and G. M. Johnson (CSIRO, Melbourne), pp. 393-408.
- Jeffries, H. E. (1991): "UNC Solar Radiation Models," unpublished draft report for EPA Cooperative Agreements CR813107, CR813964 and CR815779".

- Jeffries, H. E., K. G. Sexton, J. R. Arnold, and T. L. Kale (1989): "Validation Testing of New Mechanisms with Outdoor Chamber Data. Volume 2: Analysis of VOC Data for the CB4 and CAL Photochemical Mechanisms," Final Report, EPA-600/3-89-010b.
- Jeffries, H. E. and R. Crouse (1991): "Scientific and Technical Issues Related to the Application of Incremental Reactivity. Part II: Explaining Mechanism Differences," Report prepared for Western States Petroleum Association, Glendale, CA, October.
- Kwok, E. S. C., and R. Atkinson (1995): "Estimation of Hydroxyl Radical Reaction Rate Constants for Gas-Phase Organic Compounds Using a Structure-Reactivity Relationship: An Update," *Atmos. Environ* 29, 1685-1695.
- Lurmann, F. W. and H. H. Main (1992): "Analysis of the Ambient VOC Data Collected in the Southern California Air Quality Study," Final Report to California Air Resources Board Contract No. A832-130, February.
- McBride, S., M. Oravetz, and A.G. Russell. 1997. "Cost-Benefit and Uncertainty Issues Using Organic Reactivity to Regulate Urban Ozone." *Environ. Sci. Technol.* 35, A238-44.
- RRWG (1999): "VOC Reactivity Policy White Paper," Prepared by the Reactivity Research Work Group Policy Team, October 1. Available at <http://www.cgenv.com/Narsto/reactinfo.html>.
- Shi, J. and M. J. Bernhard (1997): "Kinetic Studies Of Cl-Atom Reactions with Selected Aromatic Compounds Using the Photochemical Reactor-FTIR Spectroscopy Technique," *Int. J. Chem. Kinet.* 29, 349-358.
- Sidebottom, H. W., G. LeBras, K. H. Becker, J. Wegner, E. Porter, S. O'Donnell, J. Morarity, E. Collins, A. Mellouki, S. Le Calve, I. Barnes, C. Sauer, K. Wirtz, M. Martin-Revejo, L. Theuner and J. Bea (1997): "Kinetics and Mechanisms for the Reaction of Hydroxyl Radicals with CH₃OCH₂OCH₃ and Related Compounds," Final Report to Lambiotte & Cie, S.A., September.
- Tuazon, E. C., S. M. Aschmann, R. Atkinson, and W. P. L. Carter (1998): "The reactions of Selected Acetates with the OH radical in the Presence of NO: Novel Rearrangement of Alkoxy Radicals of Structure RC(O)OCH(O.)R", *J. Phys. Chem A* 102, 2316-2321.
- Wang, L, J. B. Milford, and W. P. L. Carter (2000): "Reactivity Estimates for Aromatic Compounds 2. Uncertainty in Incremental Reactivities," *Atmos. Environ.* 34, 4349-4360.
- Wollenhaupt, M, S. A. Carl, A. Horowitz, and J. N. Crowley (2000): "Rate Coefficients for Reaction of OH with Acetone between 202 and 395 K," *J. Phys. Chem. A* 2000, 104, 2695-2705.
- Zafonte, L., P. L. Rieger, and J. R. Holmes (1977): "Nitrogen Dioxide Photolysis in the Los Angeles Atmosphere," *Environ. Sci. Technol.* 11, 483-487.

APPENDIX A.

MECHANISM LISTING AND TABULATIONS

This Appendix gives a complete listing of the mechanisms used in the model simulations in this report. Table A-1 contains a list of all the model species used in the mechanism, and Table A-2 lists the reactions and rate parameters, and Table A-3 lists the absorption cross sections and quantum yields for the photolysis reactions. In addition, Finally, Table A-4 gives the chamber-dependent parameters used in the model simulations of the chamber experiments.

Table A-1. Listing of the model species in the mechanism used in the model simulations discussed in this report.

Type and Name	Description
<u>Species used in Base Mechanism</u>	
<u>Constant Species.</u>	
O2	Oxygen
M	Air
H2O	Water
H2	Hydrogen Molecules
HV	Light
<u>Active Inorganic Species.</u>	
O3	Ozone
NO	Nitric Oxide
NO2	Nitrogen Dioxide
NO3	Nitrate Radical
N2O5	Nitrogen Pentoxide
HONO	Nitrous Acid
HNO3	Nitric Acid
HNO4	Peroxynitric Acid
HO2H	Hydrogen Peroxide
CO	Carbon Monoxide
SO2	Sulfur Dioxide
<u>Active Radical Species and Operators.</u>	
HO.	Hydroxyl Radicals
HO2.	Hydroperoxide Radicals
C-O2.	Methyl Peroxy Radicals
RO2-R.	Peroxy Radical Operator representing NO to NO2 conversion with HO2 formation.
R2O2.	Peroxy Radical Operator representing NO to NO2 conversion without HO2 formation.
RO2-N.	Peroxy Radical Operator representing NO consumption with organic nitrate formation.
CCO-O2.	Acetyl Peroxy Radicals
RCO-O2.	Peroxy Propionyl and higher peroxy acyl Radicals
BZCO-O2.	Peroxyacyl radical formed from Aromatic Aldehydes
MA-RCO3.	Peroxyacyl radicals formed from methacrolein and other acroleins.
<u>Steady State Radical Species</u>	
O3P	Ground State Oxygen Atoms
O*1D2	Excited Oxygen Atoms
TBU-O.	t-Butoxy Radicals
BZ-O.	Phenoxy Radicals
BZ(NO2)-O.	Nitro-substituted Phenoxy Radical
HOCOO.	Radical formed when Formaldehyde reacts with HO2
<u>PAN and PAN Analogues</u>	
PAN	Peroxy Acetyl Nitrate
PAN2	PPN and other higher alkyl PAN analogues
PBZN	PAN analogues formed from Aromatic Aldehydes
MA-PAN	PAN analogue formed from Methacrolein

Table A-1 (continued)

Type and Name	Description
<u>Explicit and Lumped Molecule Reactive Organic Product Species</u>	
HCHO	Formaldehyde
CCHO	Acetaldehyde
RCHO	Lumped C3+ Aldehydes
ACET	Acetone
MEK	Ketones and other non-aldehyde oxygenated products that react with OH radicals slower than $5 \times 10^{-12} \text{ cm}^3 \text{ molec}^{-2} \text{ sec}^{-1}$.
MEOH	Methanol
COOH	Methyl Hydroperoxide
ROOH	Lumped higher organic hydroperoxides
GLY	Glyoxal
MGLY	Methyl Glyoxal
BACL	Biacetyl
PHEN	Phenol
CRES	Cresols
NPHE	Nitrophenols
BALD	Aromatic aldehydes (e.g., benzaldehyde)
METHACRO	Methacrolein
MVK	Methyl Vinyl Ketone
ISO-PROD	Lumped isoprene product species
<u>Lumped Parameter Products</u>	
PROD2	Ketones and other non-aldehyde oxygenated products that react with OH radicals faster than $5 \times 10^{-12} \text{ cm}^3 \text{ molec}^{-2} \text{ sec}^{-1}$.
RNO3	Lumped Organic Nitrates
<u>Uncharacterized Reactive Aromatic Ring Fragmentation Products</u>	
DCB1	Reactive Aromatic Fragmentation Products that do not undergo significant photodecomposition to radicals.
DCB2	Reactive Aromatic Fragmentation Products which photolyze with alpha-dicarbonyl-like action spectrum.
DCB3	Reactive Aromatic Fragmentation Products which photolyze with acrolein action spectrum.
<u>Non-Reacting Species</u>	
CO2	Carbon Dioxide
XC	Lost Carbon
XN	Lost Nitrogen
SULF	Sulfates (SO_3 or H_2SO_4)
<u>Low Reactivity Compounds or Unknown Products Represented as Unreactive</u>	
H2	Hydrogen
HCOOH	Formic Acid
CCO-OH	Acetic Acid
RCO-OH	Higher organic acids
CCO-OOH	Peroxy Acetic Acid
RCO-OOH	Higher organic peroxy acids
NROG	Unspecified Unreactive Carbon

Table A-1 (continued)

Type and Name	Description
<u>Base ROG VOC Species and Test Compounds Used in the Chamber Simulations</u>	
N-C4	n-Butane
N-C6	n-Hexane
N-C8	n-Octane
ETHENE	Ethene
PROPENE	Propene
T-2-BUTE	<i>Trans</i> -2-Butene
TOLUENE	Toluene
M-XYLENE	m-Xylene
DMC	Dimethyl Carbonate
MIPR-CB	Methyl Isopropyl Carbonate
<u>Explicit and Lumped VOC Species used in the Ambient Simulations</u>	
<u>Primary Organics Represented explicitly</u>	
CH4	Methane
ETHENE	Ethene
ISOPRENE	Isoprene
<u>Example Test VOCs not in the Base Mechanism</u>	
ETHANE	Ethane
<u>Lumped Parameter Species</u>	
ALK1	Alkanes and other non-aromatic compounds that react only with OH, and have $k_{OH} < 5 \times 10^2$ ppm-1 min-1. (Primarily ethane)
ALK2	Alkanes and other non-aromatic compounds that react only with OH, and have k_{OH} between 5×10^2 and 2.5×10^3 ppm-1 min-1. (Primarily propane and acetylene)
ALK3	Alkanes and other non-aromatic compounds that react only with OH, and have k_{OH} between 2.5×10^3 and 5×10^3 ppm-1 min-1.
ALK4	Alkanes and other non-aromatic compounds that react only with OH, and have k_{OH} between 5×10^3 and 1×10^4 ppm-1 min-1.
ALK5	Alkanes and other non-aromatic compounds that react only with OH, and have k_{OH} greater than 1×10^4 ppm-1 min-1.
ARO1	Aromatics with $k_{OH} < 2 \times 10^4$ ppm-1 min-1.
ARO2	Aromatics with $k_{OH} > 2 \times 10^4$ ppm-1 min-1.
OLE1	Alkenes (other than ethene) with $k_{OH} < 7 \times 10^4$ ppm-1 min-1.
OLE2	Alkenes with $k_{OH} > 7 \times 10^4$ ppm-1 min-1.
TERP	Terpenes

Table A-2. Listing of the reactions in the mechanism used in the model simulations discussed in this report. See Carter (2000) for documentation.

Label	Rate Parameters [a]				Reaction and Products [b]
	k(298)	A	Ea	B	
<u>Inorganic Reactions</u>					
1		Phot Set= NO2			NO2 + HV = NO + O3P
2	5.79e-34	5.68e-34	0.00	-2.8	O3P + O2 + M = O3 + M
3	7.96e-15	8.00e-12	4.09		O3P + O3 = #2 O2
4	1.01e-31	1.00e-31	0.00	-1.6	O3P + NO + M = NO2 + M
5	9.72e-12	6.50e-12	-0.24		O3P + NO2 = NO + O2
6	1.82e-12	Falloff, F=0.80			O3P + NO2 = NO3 + M
		0: 9.00e-32	0.00	-2.0	
		inf: 2.20e-11	0.00	0.0	
8	1.81e-14	1.80e-12	2.72		O3 + NO = NO2 + O2
9	3.52e-17	1.40e-13	4.91		O3 + NO2 = O2 + NO3
10	2.60e-11	1.80e-11	-0.22		NO + NO3 = #2 NO2
11	1.95e-38	3.30e-39	-1.05		NO + NO + O2 = #2 NO2
12	1.54e-12	Falloff, F=0.45			NO2 + NO3 = N2O5
		0: 2.80e-30	0.00	-3.5	
		inf: 2.00e-12	0.00	0.2	
13	5.28e-2	Falloff, F=0.45			N2O5 = NO2 + NO3
		0: 1.00e-3	21.86	-3.5	
		inf: 9.70e+14	22.02	0.1	
14	2.60e-22	2.60e-22			N2O5 + H2O = #2 HNO3
15		(Slow)			N2O5 + HV = NO3 + NO + O3P
16		(Slow)			N2O5 + HV = NO3 + NO2
17	6.56e-16	4.50e-14	2.50		NO2 + NO3 = NO + NO2 + O2
18		Phot Set= NO3NO			NO3 + HV = NO + O2
19		Phot Set= NO3NO2			NO3 + HV = NO2 + O3P
20		Phot Set= O3O3P			O3 + HV = O3P + O2
21		Phot Set= O3O1D			O3 + HV = O*1D2 + O2
22	2.20e-10	2.20e-10			O*1D2 + H2O = #2 HO.
23	2.87e-11	2.09e-11	-0.19		O*1D2 + M = O3P + M
24	7.41e-12	Falloff, F=0.60			HO. + NO = HONO
		0: 7.00e-31	0.00	-2.6	
		inf: 3.60e-11	0.00	-0.1	
25		Phot Set= HONO-NO			HONO + HV = HO. + NO
26		Phot Set= HONO-NO2			HONO + HV = HO2. + NO2
27	6.46e-12	2.70e-12	-0.52		HO. + HONO = H2O + NO2
28	8.98e-12	Falloff, F=0.60			HO. + NO2 = HNO3
		0: 2.43e-30	0.00	-3.1	
		inf: 1.67e-11	0.00	-2.1	
29	2.00e-11	2.00e-11			HO. + NO3 = HO2. + NO2
30	1.47e-13	k = k0+k3M/(1+k3M/k2)			HO. + HNO3 = H2O + NO3
		k0: 7.20e-15	-1.56	0.0	
		k2: 4.10e-16	-2.86	0.0	
		k3: 1.90e-33	-1.44	0.0	
31		Phot Set= HNO3			HNO3 + HV = HO. + NO2
32	2.09e-13	k = k1 + k2 [M]			HO. + CO = HO2. + CO2
		k1: 1.30e-13	0.00	0.0	
		k2: 3.19e-33	0.00	0.0	
33	6.63e-14	1.90e-12	1.99		HO. + O3 = HO2. + O2

Table A-2 (continued)

Label	Rate Parameters [a]				Reaction and Products [b]
	k(298)	A	Ea	B	
34	8.41e-12	3.40e-12	-0.54		HO2. + NO = HO. + NO2
35	1.38e-12	Falloff, F=0.60			HO2. + NO2 = HNO4
		0:	1.80e-31	0.00	-3.2
		inf:	4.70e-12	0.00	0.0
36	7.55e-2	Falloff, F=0.50			HNO4 = HO2. + NO2
		0:	4.10e-5	21.16	0.0
		inf:	5.70e+15	22.20	0.0
37		Phot Set= HO2NO2			HNO4 + HV = #.61 {HO2. + NO2} + #.39 {HO. + NO3}
38	5.02e-12	1.50e-12	-0.72		HNO4 + HO. = H2O + NO2 + O2
39	1.87e-15	1.40e-14	1.19		HO2. + O3 = HO. + #2 O2
40A	2.87e-12	k = k1 + k2 [M]			HO2. + HO2. = HO2H + O2
		k1:	2.20e-13	-1.19	0.0
		k2:	1.85e-33	-1.95	0.0
40B	6.46e-30	k = k1 + k2 [M]			HO2. + HO2. + H2O = HO2H + O2 + H2O
		k1:	3.08e-34	-5.56	0.0
		k2:	2.59e-54	-6.32	0.0
41	4.00e-12	4.00e-12			NO3 + HO2. = #.8 {HO. + NO2 + O2} + #.2 {HNO3 + O2}
42	2.28e-16	8.50e-13	4.87		NO3 + NO3 = #2 NO2 + O2
43		Phot Set= H2O2			HO2H + HV = #2 HO.
44	1.70e-12	2.90e-12	0.32		HO2H + HO. = HO2. + H2O
45	1.11e-10	4.80e-11	-0.50		HO. + HO2. = H2O + O2
S2OH	9.77e-13	Falloff, F=0.45			HO. + SO2 = HO2. + SULF
		0:	4.00e-31	0.00	-3.3
		inf:	2.00e-12	0.00	0.0
H2OH	6.70e-15	7.70e-12	4.17		HO. + H2 = HO2. + H2O
<u>Methyl peroxy and methoxy reactions</u>					
MER1	7.29e-12	2.80e-12	-0.57		C-O2. + NO = NO2 + HCHO + HO2.
MER4	5.21e-12	3.80e-13	-1.55		C-O2. + HO2. = COOH + O2
MEN3	1.30e-12	1.30e-12			C-O2. + NO3 = HCHO + HO2. + NO2
MER5	2.65e-13	2.45e-14	-1.41		C-O2. + C-O2. = MEOH + HCHO + O2
MER6	1.07e-13	5.90e-13	1.01		C-O2. + C-O2. = #2 {HCHO + HO2.}
<u>Peroxy Radical Operators</u>					
RRNO	9.04e-12	2.70e-12	-0.72		RO2-R. + NO = NO2 + HO2.
RRH2	1.49e-11	1.90e-13	-2.58		RO2-R. + HO2. = ROOH + O2 + #-3 XC
RRN3	2.30e-12	2.30e-12			RO2-R. + NO3 = NO2 + O2 + HO2.
RRME	2.00e-13	2.00e-13			RO2-R. + C-O2. = HO2. + #.75 HCHO + #.25 MEOH
RRR2	3.50e-14	3.50e-14			RO2-R. + RO2-R. = HO2.
R2NO	Same k as rxn RRNO				R2O2. + NO = NO2
R2H2	Same k as rxn RRH2				R2O2. + HO2. = HO2.
R2N3	Same k as rxn RRN3				R2O2. + NO3 = NO2
R2ME	Same k as rxn RRME				R2O2. + C-O2. = C-O2.
R2RR	Same k as rxn RRR2				R2O2. + RO2-R. = RO2-R.
R2R3	Same k as rxn RRR2				R2O2. + R2O2. =
RNNO	Same k as rxn RRNO				RO2-N. + NO = RNO3
RNH2	Same k as rxn RRH2				RO2-N. + HO2. = ROOH + #3 XC
RNME	Same k as rxn RRME				RO2-N. + C-O2. = HO2. + #.25 MEOH + #.5 {MEK + PROD2} + #.75 HCHO + XC
RNN3	Same k as rxn RRN3				RO2-N. + NO3 = NO2 + O2 + HO2. + MEK + #2 XC

Table A-2 (continued)

Label	Rate Parameters [a]			B	Reaction and Products [b]
	k(298)	A	Ea		
RNR2		Same k as rxn RRR2			RO2-N. + RO2-R. = HO2. + #.5 {MEK + PROD2} + O2 + XC
RNR2		Same k as rxn RRR2			RO2-N. + R2O2. = RO2-N.
RNRN		Same k as rxn RRR2			RO2-N. + RO2-N. = MEK + HO2. + PROD2 + O2 + #2 XC
APN2	1.05e-11	Falloff, F=0.30			CCO-O2. + NO2 = PAN
		0:	2.70e-28	0.00	-7.1
		inf:	1.20e-11	0.00	-0.9
DPAN	5.21e-4	Falloff, F=0.30			PAN = CCO-O2. + NO2
		0:	4.90e-3	24.05	0.0
		inf:	4.00e+16	27.03	0.0
APNO	2.13e-11	7.80e-12	-0.60		CCO-O2. + NO = C-O2. + CO2 + NO2
APH2	1.41e-11	4.30e-13	-2.07		CCO-O2. + HO2. = #.75 {CCO-OOH + O2} + #.25 {CCO-OH + O3}
APN3	4.00e-12	4.00e-12			CCO-O2. + NO3 = C-O2. + CO2 + NO2 + O2
APME	9.64e-12	1.80e-12	-0.99		CCO-O2. + C-O2. = CCO-OH + HCHO + O2
APRR	7.50e-12	7.50e-12			CCO-O2. + RO2-R. = CCO-OH
APR2		Same k as rxn APRR			CCO-O2. + R2O2. = CCO-O2.
APRN		Same k as rxn APRR			CCO-O2. + RO2-N. = CCO-OH + PROD2
APAP	1.55e-11	2.90e-12	-0.99		CCO-O2. + CCO-O2. = #2 {C-O2. + CO2} + O2
PPN2	1.21e-11	1.20e-11	0.00	-0.9	RCO-O2. + NO2 = PAN2
PAN2	4.43e-4	2.00e+15	25.44		PAN2 = RCO-O2. + NO2
PPNO	2.80e-11	1.25e-11	-0.48		RCO-O2. + NO = NO2 + CCHO + RO2-R. + CO2
PPH2		Same k as rxn APH2			RCO-O2. + HO2. = #.75 {RCO-OOH + O2} + #.25 {RCO-OH + O3}
PPN3		Same k as rxn APN3			RCO-O2. + NO3 = NO2 + CCHO + RO2-R. + CO2 + O2
PPME		Same k as rxn APME			RCO-O2. + C-O2. = RCO-OH + HCHO + O2
PPRR		Same k as rxn APRR			RCO-O2. + RO2-R. = RCO-OH + O2
PPR2		Same k as rxn APRR			RCO-O2. + R2O2. = RCO-O2.
PPRN		Same k as rxn APRR			RCO-O2. + RO2-N. = RCO-OH + PROD2 + O2
PPAP		Same k as rxn APAP			RCO-O2. + CCO-O2. = #2 CO2 + C-O2. + CCHO + RO2-R. + O2
PPPP		Same k as rxn APAP			RCO-O2. + RCO-O2. = #2 {CCHO + RO2-R. + CO2}
BPN2	1.37e-11	1.37e-11			BZCO-O2. + NO2 = PBZN
BPAN	3.12e-4	7.90e+16	27.82		PBZN = BZCO-O2. + NO2
BPNO		Same k as rxn PPNO			BZCO-O2. + NO = NO2 + CO2 + BZ-O. + R2O2.
BPH2		Same k as rxn APH2			BZCO-O2. + HO2. = #.75 {RCO-OOH + O2} + #.25 {RCO-OH + O3} + #4 XC
BPN3		Same k as rxn APN3			BZCO-O2. + NO3 = NO2 + CO2 + BZ-O. + R2O2. + O2
BPME		Same k as rxn APME			BZCO-O2. + C-O2. = RCO-OH + HCHO + O2 + #4 XC
BPRR		Same k as rxn APRR			BZCO-O2. + RO2-R. = RCO-OH + O2 + #4 XC
BPR2		Same k as rxn APRR			BZCO-O2. + R2O2. = BZCO-O2.
BPRN		Same k as rxn APRR			BZCO-O2. + RO2-N. = RCO-OH + PROD2 + O2 + #4 XC
BPAP		Same k as rxn APAP			BZCO-O2. + CCO-O2. = #2 CO2 + C-O2. + BZ-O. + R2O2.
BPPP		Same k as rxn APAP			BZCO-O2. + RCO-O2. = #2 CO2 + CCHO + RO2-R. + BZ-O. + R2O2.
BPBP		Same k as rxn APAP			BZCO-O2. + BZCO-O2. = #2 {BZ-O. + R2O2. + CO2}
MPN2		Same k as rxn PPN2			MA-RCO3. + NO2 = MA-PAN
MPPN	3.55e-4	1.60e+16	26.80		MA-PAN = MA-RCO3. + NO2
MPNO		Same k as rxn PPNO			MA-RCO3. + NO = NO2 + CO2 + HCHO + CCO-O2.
MPH2		Same k as rxn APH2			MA-RCO3. + HO2. = #.75 {RCO-OOH + O2} + #.25 {RCO-OH + O3} + XC

Table A-2 (continued)

Label	Rate Parameters [a]			B	Reaction and Products [b]
	k(298)	A	Ea		
MPN3	Same k as rxn APN3				MA-RCO3. + NO3 = NO2 + CO2 + HCHO + CCO-O2. + O2
MPME	Same k as rxn APME				MA-RCO3. + C-O2. = RCO-OH + HCHO + XC + O2
MPRR	Same k as rxn APRR				MA-RCO3. + RO2-R. = RCO-OH + XC
MPR2	Same k as rxn APRR				MA-RCO3. + R2O2. = MA-RCO3.
MPRN	Same k as rxn APRR				MA-RCO3. + RO2-N. = #2 RCO-OH + O2 + #4 XC
MPAP	Same k as rxn APAP				MA-RCO3. + CCO-O2. = #2 CO2 + C-O2. + HCHO + CCO-O2. + O2
MPPP	Same k as rxn APAP				MA-RCO3. + RCO-O2. = HCHO + CCO-O2. + CCHO + RO2-R. + #2 CO2
MPBP	Same k as rxn APAP				MA-RCO3. + BZCO-O2. = HCHO + CCO-O2. + BZ-O. + R2O2. + #2 CO2
MPMP	Same k as rxn APAP				MA-RCO3. + MA-RCO3. = #2 {HCHO + CCO-O2. + CO2}
<u>Other Organic Radical Species</u>					
TBON	2.40e-11	2.40e-11			TBU-O. + NO2 = RNO3 + #-2 XC
TBOD	9.87e+2	7.50e+14	16.20		TBU-O. = ACET + C-O2.
BRN2	3.80e-11	2.30e-11	-0.30		BZ-O. + NO2 = NPHE
BRH2	Same k as rxn RRH2				BZ-O. + HO2. = PHEN
BRXX	1.00e-3	1.00e-3			BZ-O. = PHEN
BNN2	Same k as rxn BRN2				BZ(NO2)-O. + NO2 = #2 XN + #6 XC
BNH2	Same k as rxn RRH2				BZ(NO2)-O. + HO2. = NPHE
BNXX	Same k as rxn BRXX				BZ(NO2)-O. = NPHE
<u>Explicit and Lumped Molecule Organic Products</u>					
FAHV	Phot Set= HCHO_R				HCHO + HV = #2 HO2. + CO
FAVS	Phot Set= HCHO_M				HCHO + HV = H2 + CO
FAOH	9.20e-12	8.60e-12	-0.04		HCHO + HO. = HO2. + CO + H2O
FAH2	7.90e-14	9.70e-15	-1.24		HCHO + HO2. = HOCOO.
FAHR	1.51e+2	2.40e+12	13.91		HOCOO. = HO2. + HCHO
FAHN	Same k as rxn MER1				HOCOO. + NO = HCOOH + NO2 + HO2.
FAN3	5.74e-16	2.00e-12	4.83		HCHO + NO3 = HNO3 + HO2. + CO
AAOH	1.58e-11	5.60e-12	-0.62		CCHO + HO. = CCO-O2. + H2O
AAHV	Phot Set= CCHO_R				CCHO + HV = CO + HO2. + C-O2.
AAN3	2.73e-15	1.40e-12	3.70		CCHO + NO3 = HNO3 + CCO-O2.
PAOH	2.00e-11	2.00e-11			RCHO + HO. = #.034 RO2-R. + #.001 RO2-N. + #.965 RCO-O2. + #.034 CO + #.034 CCHO + #.0003 XC
PAHV	Phot Set= C2CHO				RCHO + HV = CCHO + RO2-R. + CO + HO2.
PAN3	3.67e-15	1.40e-12	3.52		RCHO + NO3 = HNO3 + RCO-O2.
K3OH	1.92e-13	1.10e-12	1.03		ACET + HO. = HCHO + CCO-O2. + R2O2.
K3HV	Phot Set= ACETONE				ACET + HV = CCO-O2. + C-O2.
K4OH	1.18e-12	1.30e-12	0.05	2.0	MEK + HO. = #.37 RO2-R. + #.042 RO2-N. + #.616 R2O2. + #.492 CCO-O2. + #.096 RCO-O2. + #.115 HCHO + #.482 CCHO + #.37 RCHO + #.287 XC
K4HV	Phot Set= KETONE, qy= 1.5e-1				MEK + HV = CCO-O2. + CCHO + RO2-R.
MeOH	9.14e-13	3.10e-12	0.72	2.0	MEOH + HO. = HCHO + HO2.
MER9	5.49e-12	2.90e-12	-0.38		COOH + HO. = H2O + #.35 {HCHO + HO.} + #.65 C-O2.
MERA	Phot Set= COOH				COOH + HV = HCHO + HO2. + HO.

Table A-2 (continued)

Label	Rate Parameters [a]				Reaction and Products [b]
	k(298)	A	Ea	B	
LPR9	1.10e-11	1.10e-11			ROOH + HO. = H2O + RCHO + #.34 RO2-R. + #.66 HO.
LPRA		Phot Set= COOH			ROOH + HV = RCHO + HO2. + HO.
GLHV		Phot Set= GLY_R			GLY + HV = #2 {CO + HO2.}
GLVM		Phot Set= GLY_ABS, qy= 6.0e-3			GLY + HV = HCHO + CO
GLOH	1.10e-11	1.10e-11			GLY + HO. = #.63 HO2. + #1.26 CO + #.37 RCO-O2. + #-.37 XC
GLN3	9.63e-16	2.80e-12	4.72		GLY + NO3 = HNO3 + #.63 HO2. + #1.26 CO + #.37 RCO-O2. + #-.37 XC
MGHV		Phot Set= MGLY_ADJ			MGLY + HV = HO2. + CO + CCO-O2.
MGOH	1.50e-11	1.50e-11			MGLY + HO. = CO + CCO-O2.
MGN3	2.43e-15	1.40e-12	3.77		MGLY + NO3 = HNO3 + CO + CCO-O2.
BAHV		Phot Set= BAACL_ADJ			BAACL + HV = #2 CCO-O2.
PHOH	2.63e-11	2.63e-11			PHEN + HO. = #.24 BZ-O. + #.76 RO2-R. + #.23 GLY + #4.1 XC
PHN3	3.78e-12	3.78e-12			PHEN + NO3 = HNO3 + BZ-O.
CROH	4.20e-11	4.20e-11			CRES + HO. = #.24 BZ-O. + #.76 RO2-R. + #.23 MGLY + #4.87 XC
CRN3	1.37e-11	1.37e-11			CRES + NO3 = HNO3 + BZ-O. + XC
NPN3		Same k as rxn PHN3			NPHE + NO3 = HNO3 + BZ(NO2)-O.
BZOH	1.29e-11	1.29e-11			BALD + HO. = BZCO-O2.
BZHV		Phot Set= BZCHO, qy= 5.0e-2			BALD + HV = #7 XC
BZNT	2.62e-15	1.40e-12	3.72		BALD + NO3 = HNO3 + BZCO-O2.
MAOH	3.36e-11	1.86e-11	-0.35		METHACRO + HO. = #.5 RO2-R. + #.416 CO + #.084 HCHO + #.416 MEK + #.084 MGLY + #.5 MA-RCO3. + #-.0416 XC
MAO3	1.13e-18	1.36e-15	4.20		METHACRO + O3 = #.008 HO2. + #.1 RO2-R. + #.208 HO. + #.1 RCO-O2. + #.45 CO + #.117 CO2 + #.2 HCHO + #.9 MGLY + #.333 HCOOH + #-.0.1 XC
MAN3	4.58e-15	1.50e-12	3.43		METHACRO + NO3 = #.5 {HNO3 + RO2-R. + CO + MA-RCO3.} + #1.5 XC + #.5 XN
MAOP	6.34e-12	6.34e-12			METHACRO + O3P = RCHO + XC
MAHV		Phot Set= ACROLEIN, qy= 4.1e-3			METHACRO + HV = #.34 HO2. + #.33 RO2-R. + #.33 HO. + #.67 CCO-O2. + #.67 CO + #.67 HCHO + #.33 MA-RCO3. + #-.0 XC
MVOH	1.89e-11	4.14e-12	-0.90		MVK + HO. = #.3 RO2-R. + #.025 RO2-N. + #.675 R2O2. + #.675 CCO-O2. + #.3 HCHO + #.675 RCHO + #.3 MGLY + #-.0.725 XC
MVO3	4.58e-18	7.51e-16	3.02		MVK + O3 = #.064 HO2. + #.05 RO2-R. + #.164 HO. + #.05 RCO-O2. + #.475 CO + #.124 CO2 + #.1 HCHO + #.95 MGLY + #.351 HCOOH + #-.0.05 XC
MVN3		(Slow)			MVK + NO3 = #4 XC + XN
MVOP	4.32e-12	4.32e-12			MVK + O3P = #.45 RCHO + #.55 MEK + #.45 XC
MVHV		Phot Set= ACROLEIN, qy= 2.1e-3			MVK + HV = #.3 C-O2. + #.7 CO + #.7 PROD2 + #.3 MA-RCO3. + #-.2.4 XC
IPOH	6.19e-11	6.19e-11			ISO-PROD + HO. = #.67 RO2-R. + #.041 RO2-N. + #.289 MA-RCO3. + #.336 CO + #.055 HCHO + #.129 CCHO + #.013 RCHO + #.15 MEK + #.332 PROD2 + #.15 GLY + #.174 MGLY + #-.0.504 XC

Table A-2 (continued)

Label	Rate Parameters [a]				Reaction and Products [b]
	k(298)	A	Ea	B	
IPO3	4.18e-18	4.18e-18			ISO-PROD + O3 = #.4 HO2. + #.048 RO2-R. + #.048 RCO-O2. + #.285 HO. + #.498 CO + #.14 CO2 + #.125 HCHO + #.047 CCHO + #.21 MEK + #.023 GLY + #.742 MGLY + #.1 HCOOH + #.372 RCO-OH + #.33 XC
IPN3	1.00e-13	1.00e-13			ISO-PROD + NO3 = #.799 RO2-R. + #.051 RO2-N. + #.15 MA-RCO3. + #.572 CO + #.15 HNO3 + #.227 HCHO + #.218 RCHO + #.008 MGLY + #.572 RNO3 + #.28 XN + #.815 XC
IPHV	Phot Set= ACROLEIN, qy= 4.1e-3				ISO-PROD + HV = #1.233 HO2. + #.467 CCO-O2. + #.3 RCO-O2. + #1.233 CO + #.3 HCHO + #.467 CCHO + #.233 MEK + #.233 XC
<u>Lumped Parameter Organic Products</u>					
K6OH	1.50e-11	1.50e-11			PROD2 + HO. = #.379 HO2. + #.473 RO2-R. + #.07 RO2-N. + #.029 CCO-O2. + #.049 RCO-O2. + #.213 HCHO + #.084 CCHO + #.558 RCHO + #.115 MEK + #.329 PROD2 + #.886 XC
K6HV	Phot Set= KETONE, qy= 2.0e-2				PROD2 + HV = #.96 RO2-R. + #.04 RO2-N. + #.515 R2O2. + #.667 CCO-O2. + #.333 RCO-O2. + #.506 HCHO + #.246 CCHO + #.71 RCHO + #.299 XC
RNOH	7.80e-12	7.80e-12			RNO3 + HO. = #.338 NO2 + #.113 HO2. + #.376 RO2-R. + #.173 RO2-N. + #.596 R2O2. + #.01 HCHO + #.439 CCHO + #.213 RCHO + #.006 ACET + #.177 MEK + #.048 PROD2 + #.31 RNO3 + #.351 XN + #.56 XC
RNHV	Phot Set= IC3ONO2				RNO3 + HV = NO2 + #.341 HO2. + #.564 RO2-R. + #.095 RO2-N. + #.152 R2O2. + #.134 HCHO + #.431 CCHO + #.147 RCHO + #.02 ACET + #.243 MEK + #.435 PROD2 + #.35 XC
<u>Uncharacterized Reactive Aromatic Ring Fragmentation Products</u>					
D1OH	5.00e-11	5.00e-11			DCB1 + HO. = RCHO + RO2-R. + CO
D1HV			(Slow)		DCB1 + HV = HO2. + #2 CO + RO2-R. + GLY + R2O2.
D1O3	2.00e-18	2.00e-18			DCB1 + O3 = #1.5 HO2. + #.5 HO. + #1.5 CO + #.5 CO2 + GLY
D2OH	5.00e-11	5.00e-11			DCB2 + HO. = R2O2. + RCHO + CCO-O2.
D2HV	Phot Set= MGLY_ABS, qy= 3.7e-1				DCB2 + HV = RO2-R. + #.5 {CCO-O2. + HO2.} + CO + R2O2. + #.5 {GLY + MGLY + XC}
D3OH	5.00e-11	5.00e-11			DCB3 + HO. = R2O2. + RCHO + CCO-O2.
D3HV	Phot Set= ACROLEIN, qy= 7.3e+0				DCB3 + HV = RO2-R. + #.5 {CCO-O2. + HO2.} + CO + R2O2. + #.5 {GLY + MGLY + XC}
<u>Base ROG VOCs Used in the Chamber Simulations and Explicit VOCs in the Ambient Simulations</u>					
c1OH	6.37e-15	2.15e-12	3.45		CH4 + HO. = H2O + C-O2.
c2OH	2.54e-13	1.37e-12	0.99	2.0	ETHANE + HO. = RO2-R. + CCHO
c4OH	2.44e-12	1.52e-12	-0.29	2.0	N-C4 + HO. = #.921 RO2-R. + #.079 RO2-N. + #.413 R2O2. + #.632 CCHO + #.12 RCHO + #.485 MEK + #.038 XC
c6OH	5.47e-12	1.38e-12	-0.82	2.0	N-C6 + HO. = #.775 RO2-R. + #.225 RO2-N. + #.787 R2O2. + #.011 CCHO + #.113 RCHO + #.688 PROD2 + #.162 XC
c8OH	8.70e-12	2.48e-12	-0.75	2.0	N-C8 + HO. = #.646 RO2-R. + #.354 RO2-N. + #.786 R2O2. + #.024 RCHO + #.622 PROD2 + #2.073 XC
etOH	8.52e-12	1.96e-12	-0.87		ETHENE + HO. = RO2-R. + #1.61 HCHO + #.195 CCHO
etO3	1.59e-18	9.14e-15	5.13		ETHENE + O3 = #.12 HO. + #.12 HO2. + #.5 CO + #.13 CO2 + HCHO + #.37 HCOOH
etN3	2.05e-16	4.39e-13	4.53	2.0	ETHENE + NO3 = RO2-R. + RCHO + #-1 XC + XN

Table A-2 (continued)

Label	Rate Parameters [a]			Reaction and Products [b]	
	k(298)	A	Ea		
etOA	7.29e-13	1.04e-11	1.57		ETHENE + O3P = #.5 HO2. + #.2 RO2-R. + #.3 C-O2. + #.491 CO + #.191 HCHO + #.25 CCHO + #.009 GLY + #.5 XC
prOH	2.63e-11	4.85e-12	-1.00		PROPENE + HO. = #.984 RO2-R. + #.016 RO2-N. + #.984 HCHO + #.984 CCHO + #-0.048 XC
prO3	1.01e-17	5.51e-15	3.73		PROPENE + O3 = #.32 HO. + #.06 HO2. + #.26 C-O2. + #.51 CO + #.135 CO2 + #.5 HCHO + #.5 CCHO + #.185 HCOOH + #.17 CCO-OH + #.07 INERT + #.07 XC
prN3	9.49e-15	4.59e-13	2.30		PROPENE + NO3 = #.949 RO2-R. + #.051 RO2-N. + #.2.693 XC + XN
prOP	3.98e-12	1.18e-11	0.64		PROPENE + O3P = #.45 RCHO + #.55 MEK + #-0.55 XC
t2OH	6.40e-11	1.01e-11	-1.09		T-2-BUTE + HO. = #.965 RO2-R. + #.035 RO2-N. + #1.93 CCHO + #-0.07 XC
t2O3	1.90e-16	6.64e-15	2.10		T-2-BUTE + O3 = #.52 HO. + #.52 C-O2. + #.52 CO + #.14 CO2 + CCHO + #.34 CCO-OH + #.14 INERT + #.14 XC
t2N3	3.91e-13	1.10e-13	-0.76	2.0	T-2-BUTE + NO3 = #.705 NO2 + #.215 RO2-R. + #.08 RO2-N. + #.705 R2O2. + #1.41 CCHO + #.215 RNO3 + #-0.59 XC + #.08 XN
t2OP	2.18e-11	2.18e-11			T-2-BUTE + O3P = MEK
isOH	9.82e-11	2.50e-11	-0.81		ISOPRENE + HO. = #.907 RO2-R. + #.093 RO2-N. + #.079 R2O2. + #.624 HCHO + #.23 METHACRO + #.32 MVK + #.357 ISO-PROD + #-0.167 XC
isO3	1.28e-17	7.86e-15	3.80		ISOPRENE + O3 = #.266 HO. + #.066 RO2-R. + #.008 RO2-N. + #.126 R2O2. + #.192 MA-RCO3. + #.275 CO + #.122 CO2 + #.592 HCHO + #.1 PROD2 + #.39 METHACRO + #.16 MVK + #.204 HCOOH + #.15 RCO-OH + #-0.259 XC
isN3	6.74e-13	3.03e-12	0.89		ISOPRENE + NO3 = #.187 NO2 + #.749 RO2-R. + #.064 RO2-N. + #.187 R2O2. + #.936 ISO-PROD + #-0.064 XC + #.813 XN
isOP	3.60e-11	3.60e-11			ISOPRENE + O3P = #.01 RO2-N. + #.24 R2O2. + #.25 C-O2. + #.24 MA-RCO3. + #.24 HCHO + #.75 PROD2 + #-1.01 XC
t1OH	5.95e-12	1.81e-12	-0.71	0.0	TOLUENE + HO. = #.234 HO2. + #.758 RO2-R. + #.008 RO2-N. + #.116 GLY + #.135 MGLY + #.234 CRES + #.085 BALD + #.46 DCB1 + #.156 DCB2 + #.057 DCB3 + #1.178 XC
mxOH	2.36e-11	2.36e-11	0.00	0.0	M-XYLENE + HO. = #.21 HO2. + #.782 RO2-R. + #.008 RO2-N. + #.107 GLY + #.335 MGLY + #.21 CRES + #.037 BALD + #.347 DCB1 + #.29 DCB2 + #.108 DCB3 + #1.628 XC
Lumped Organic Species used in the Ambient Reactivity Simulations					
t1OH	8.27e-11	1.83e-11	-0.89		TERP + HO. = #.75 RO2-R. + #.25 RO2-N. + #.5 R2O2. + #.276 HCHO + #.474 RCHO + #.276 PROD2 + #5.146 XC
t1O3	6.88e-17	1.08e-15	1.63		TERP + O3 = #.567 HO. + #.033 HO2. + #.031 RO2-R. + #.18 RO2-N. + #.729 R2O2. + #.123 CCO-O2. + #.201 RCO-O2. + #.157 CO + #.037 CO2 + #.235 HCHO + #.205 RCHO + #.13 ACET + #.276 PROD2 + #.001 GLY + #.031 BACL + #.103 HCOOH + #.189 RCO-OH + #4.183 XC
t1N3	6.57e-12	3.66e-12	-0.35		TERP + NO3 = #.474 NO2 + #.276 RO2-R. + #.25 RO2-N. + #.75 R2O2. + #.474 RCHO + #.276 RNO3 + #5.421 XC + #.25 XN
t1OP	3.27e-11	3.27e-11			TERP + O3P = #.147 RCHO + #.853 PROD2 + #4.441 XC
a1OH	2.54e-13	1.37e-12	0.99	2.0	ALK1 + HO. = RO2-R. + CCHO

Table A-2 (continued)

Label	Rate Parameters [a]			B	Reaction and Products [b]
	k(298)	A	Ea		
a2OH	1.04e-12	9.87e-12	1.33		ALK2 + HO. = #.246 HO. + #.121 HO2. + #.612 RO2-R. + #.021 RO2-N. + #.16 CO + #.039 HCHO + #.155 RCHO + #.417 ACET + #.248 GLY + #.121 HCOOH + #0.338 XC
a3OH	2.38e-12	1.02e-11	0.86		ALK3 + HO. = #.695 RO2-R. + #.07 RO2-N. + #.559 R2O2. + #.236 TBU-O. + #.026 HCHO + #.445 CCHO + #.122 RCHO + #.024 ACET + #.332 MEK + #-0.05 XC
a4OH	4.39e-12	5.95e-12	0.18		ALK4 + HO. = #.835 RO2-R. + #.143 RO2-N. + #.936 R2O2. + #.011 C-O2. + #.011 CCO-O2. + #.002 CO + #.024 HCHO + #.455 CCHO + #.244 RCHO + #.452 ACET + #.11 MEK + #.125 PROD2 + #-0.105 XC
a5OH	9.34e-12	1.11e-11	0.10		ALK5 + HO. = #.653 RO2-R. + #.347 RO2-N. + #.948 R2O2. + #.026 HCHO + #.099 CCHO + #.204 RCHO + #.072 ACET + #.089 MEK + #.417 PROD2 + #2.008 XC
b1OH	5.95e-12	1.81e-12	-0.71		ARO1 + HO. = #.224 HO2. + #.765 RO2-R. + #.011 RO2-N. + #.055 PROD2 + #.118 GLY + #.119 MGLY + #.017 PHEN + #.207 CRES + #.059 BALD + #.491 DCB1 + #.108 DCB2 + #.051 DCB3 + #1.288 XC
b2OH	2.64e-11	2.64e-11	0.00		ARO2 + HO. = #.187 HO2. + #.804 RO2-R. + #.009 RO2-N. + #.097 GLY + #.287 MGLY + #.087 BA CL + #.187 CRES + #.05 BALD + #.561 DCB1 + #.099 DCB2 + #.093 DCB3 + #1.68 XC
o1OH	3.23e-11	7.10e-12	-0.90		OLE1 + HO. = #.91 RO2-R. + #.09 RO2-N. + #.205 R2O2. + #.732 HCHO + #.294 CCHO + #.497 RCHO + #.005 ACET + #.119 PROD2 + #.92 XC
o1O3	1.06e-17	2.62e-15	3.26		OLE1 + O3 = #.155 HO. + #.056 HO2. + #.022 RO2-R. + #.001 RO2-N. + #.076 C-O2. + #.345 CO + #.086 CO2 + #.5 HCHO + #.154 CCHO + #.363 RCHO + #.001 ACET + #.215 PROD2 + #.185 HCOOH + #.05 CCO-OH + #.119 RCO-OH + #.654 XC
o1N3	1.26e-14	4.45e-14	0.75		OLE1 + NO3 = #.824 RO2-R. + #.176 RO2-N. + #.488 R2O2. + #.009 CCHO + #.037 RCHO + #.024 ACET + #.511 RNO3 + #.677 XC + #.489 XN
o1OP	4.90e-12	1.07e-11	0.47		OLE1 + O3P = #.45 RCHO + #.437 MEK + #.113 PROD2 + #1.224 XC
o2OH	6.33e-11	1.74e-11	-0.76		OLE2 + HO. = #.918 RO2-R. + #.082 RO2-N. + #.001 R2O2. + #.244 HCHO + #.732 CCHO + #.511 RCHO + #.127 ACET + #.072 MEK + #.061 BALD + #.025 METHACRO + #.025 ISO-PROD + #-0.054 XC
o2O3	1.07e-16	5.02e-16	0.92		OLE2 + O3 = #.378 HO. + #.003 HO2. + #.033 RO2-R. + #.002 RO2-N. + #.137 R2O2. + #.197 C-O2. + #.137 CCO-O2. + #.006 RCO-O2. + #.265 CO + #.07 CO2 + #.269 HCHO + #.456 CCHO + #.305 RCHO + #.045 ACET + #.026 MEK + #.006 PROD2 + #.042 BALD + #.026 METHACRO + #.073 HCOOH + #.129 CCO-OH + #.303 RCO-OH + #.155 XC
o2N3	7.27e-13	7.27e-13	0.00		OLE2 + NO3 = #.391 NO2 + #.442 RO2-R. + #.136 RO2-N. + #.711 R2O2. + #.03 C-O2. + #.079 HCHO + #.507 CCHO + #.151 RCHO + #.102 ACET + #.001 MEK + #.015 BALD + #.048 MVK + #.321 RNO3 + #.075 XC + #.288 XN
o2OP	2.09e-11	2.09e-11			OLE2 + O3P = #.013 HO2. + #.012 RO2-R. + #.001 RO2-N. + #.012 CO + #.069 RCHO + #.659 MEK + #.259 PROD2 + #.012 METHACRO + #.537 XC

Table A-2 (continued)

Label	Rate Parameters [a]			Reaction and Products [b]
	k(298)	A	Ea B	
<u>Test Compounds Studied for This Project [c]</u>				
	3.30e-13	3.30e-13		DMC + HO. = RO2-R. + #.393 CO + #.393 RCO-OH + #.607 INERT + #.82 XC
	2.55e-12	2.55e-12		MIPR-CB + HO. = #.302 RO2-R. + #.047 RO2-N. + #.707 R2O2. + #.599 C-O2. + #.052 CCO-O2. + #.023 CO + #.209 CO2 + #.265 HCHO + #.033 RCHO + #.209 ACET + #.035 MEK + #.075 RCO-OH + #.601 INERT + #1.825 XC

[a] Except as indicated, the rate constants are given by $k(T) = A \cdot (T/300)^B \cdot e^{-E_a/RT}$, where the units of k and A are $\text{cm}^3 \text{ molec}^{-1} \text{ s}^{-1}$, E_a are kcal mol^{-1} , T is $^{\circ}\text{K}$, and $R=0.0019872 \text{ kcal mol}^{-1} \text{ deg}^{-1}$. The following special rate constant expressions are used:

Phot Set = name: The absorption cross sections and quantum yields for the photolysis reaction are given in Table A-5, where “name” indicates the photolysis set used. If a “*qy=number*” notation is given, the number given is the overall quantum yield, which is assumed to be wavelength independent.

Falloff: The rate constant as a function of temperature and pressure is calculated using $k(T,M) = \{k_0(T) \cdot [M] / [1 + k_0(T) \cdot [M] / k_{inf}(T)]\} \cdot F^Z$, where $Z = \{1 + [\log_{10}\{k_0(T) \cdot [M] / k_{inf}(T)\}]^2\}^{-1}$, [M] is the total pressure in molecules cm^{-3} , F is as indicated on the table, and the temperature dependences of k_0 and k_{inf} are as indicated on the table.

(Slow): The reaction is assumed to be negligible and is not included in the mechanism. It is shown on the listing for documentation purposes only.

$k = k_0 + k_3M(1 + k_3M/k_2)$: The rate constant as a function of temperature and pressure is calculated using $k(T,M) = k_0(T) + k_3(T) \cdot [M] \cdot (1 + k_3(T) \cdot [M] / k_2(T))$, where [M] is the total bath gas (air) concentration in molecules cm^{-3} , and the temperature dependences for k_0 , k_2 and k_3 are as indicated on the table.

$k = k_1 + k_2 [M]$: The rate constant as a function of temperature and pressure is calculated using $k(T,M) = k_1(T) + k_2(T) \cdot [M]$, where [M] is the total bath gas (air) concentration in molecules cm^{-3} , and the temperature dependences for k_1 , and k_2 are as indicated on the table.

Same k as Rxn label: The rate constant is the same as the reaction with the indicated label.

- [b] Format of reaction listing: “=” separates reactants from products; “#number” indicates stoichiometric coefficient, “#coefficient { product list }” means that the stoichiometric coefficient is applied to all the products listed. See Table A-1 for a listing of the model species used.
- [c] Mechanisms from Carter (2000) and as discussed in this work. However, note that the current recommended mechanism for DMC involves formation of 40% CO + RCO-OH and 60% INERT, which would yield the same predicted ozone impacts to within the numerical precision of the software used.

Table A-3 (continued)

WL (nm)	Abs (cm ²)	QY	WL (nm)	Abs (cm ²)	QY	WL (nm)	Abs (cm ²)	QY	WL (nm)	Abs (cm ²)	QY	WL (nm)	Abs (cm ²)	QY
366.5	1.19e-20	1.000	367.0	1.23e-20	1.000	367.5	1.27e-20	1.000	368.0	1.31e-20	1.000	368.5	1.35e-20	1.000
369.0	1.40e-20	1.000	369.5	1.44e-20	1.000	370.0	1.47e-20	1.000	370.5	1.51e-20	1.000	371.0	1.55e-20	1.000
371.5	1.59e-20	1.000	372.0	1.64e-20	1.000	372.5	1.70e-20	1.000	373.0	1.73e-20	1.000	373.5	1.77e-20	1.000
374.0	1.81e-20	1.000	374.5	1.86e-20	1.000	375.0	1.90e-20	1.000	375.5	1.96e-20	1.000	376.0	2.02e-20	1.000
376.5	2.06e-20	1.000	377.0	2.10e-20	1.000	377.5	2.14e-20	1.000	378.0	2.18e-20	1.000	378.5	2.24e-20	1.000
379.0	2.30e-20	1.000	379.5	2.37e-20	1.000	380.0	2.42e-20	1.000	380.5	2.47e-20	1.000	381.0	2.54e-20	1.000
381.5	2.62e-20	1.000	382.0	2.69e-20	1.000	382.5	2.79e-20	1.000	383.0	2.88e-20	1.000	383.5	2.96e-20	1.000
384.0	3.02e-20	1.000	384.5	3.10e-20	1.000	385.0	3.20e-20	1.000	385.5	3.29e-20	1.000	386.0	3.39e-20	1.000
386.5	3.51e-20	1.000	387.0	3.62e-20	1.000	387.5	3.69e-20	1.000	388.0	3.70e-20	1.000	388.5	3.77e-20	1.000
389.0	3.88e-20	1.000	389.5	3.97e-20	1.000	390.0	4.03e-20	1.000	390.5	4.12e-20	1.000	391.0	4.22e-20	1.000
391.5	4.29e-20	1.000	392.0	4.30e-20	1.000	392.5	4.38e-20	1.000	393.0	4.47e-20	1.000	393.5	4.55e-20	1.000
394.0	4.56e-20	1.000	394.5	4.59e-20	1.000	395.0	4.67e-20	1.000	395.5	4.80e-20	1.000	396.0	4.87e-20	1.000
396.5	4.96e-20	1.000	397.0	5.08e-20	1.000	397.5	5.19e-20	1.000	398.0	5.23e-20	1.000	398.5	5.39e-20	1.000
399.0	5.46e-20	1.000	399.5	5.54e-20	1.000	400.0	5.59e-20	1.000	400.5	5.77e-20	1.000	401.0	5.91e-20	1.000
401.5	5.99e-20	1.000	402.0	6.06e-20	1.000	402.5	6.20e-20	1.000	403.0	6.35e-20	1.000	403.5	6.52e-20	1.000
404.0	6.54e-20	1.000	404.5	6.64e-20	1.000	405.0	6.93e-20	1.000	405.5	7.15e-20	1.000	406.0	7.19e-20	1.000
406.5	7.32e-20	1.000	407.0	7.58e-20	1.000	407.5	7.88e-20	1.000	408.0	7.97e-20	1.000	408.5	7.91e-20	1.000
409.0	8.11e-20	1.000	409.5	8.41e-20	1.000	410.0	8.53e-20	1.000	410.5	8.59e-20	1.000	411.0	8.60e-20	1.000
411.5	8.80e-20	1.000	412.0	9.04e-20	1.000	412.5	9.45e-20	1.000	413.0	9.34e-20	1.000	413.5	9.37e-20	1.000
414.0	9.63e-20	1.000	414.5	9.71e-20	1.000	415.0	9.70e-20	1.000	415.5	9.65e-20	1.000	416.0	9.69e-20	1.000
416.5	9.89e-20	1.000	417.0	1.00e-19	1.000	417.5	1.02e-19	1.000	418.0	1.00e-19	1.000	418.5	1.02e-19	1.000
419.0	1.01e-19	1.000	419.5	1.01e-19	1.000	420.0	1.03e-19	1.000	420.5	1.01e-19	1.000	421.0	1.04e-19	1.000
421.5	1.05e-19	1.000	422.0	1.06e-19	1.000	422.5	1.04e-19	1.000	423.0	1.05e-19	1.000	423.5	1.05e-19	1.000
424.0	1.01e-19	1.000	424.5	1.01e-19	1.000	425.0	1.05e-19	1.000	425.5	1.03e-19	1.000	426.0	1.02e-19	1.000
426.5	1.01e-19	1.000	427.0	9.77e-20	1.000	427.5	9.81e-20	1.000	428.0	1.00e-19	1.000	428.5	1.02e-19	1.000
429.0	9.89e-20	1.000	429.5	9.85e-20	1.000	430.0	1.04e-19	1.000	430.5	1.08e-19	1.000	431.0	1.05e-19	1.000
431.5	1.02e-19	1.000	432.0	9.64e-20	1.000	432.5	1.01e-19	1.000	433.0	1.06e-19	1.000	433.5	1.09e-19	1.000
434.0	1.04e-19	1.000	434.5	1.03e-19	1.000	435.0	1.07e-19	1.000	435.5	1.16e-19	1.000	436.0	1.09e-19	1.000
436.5	1.11e-19	1.000	437.0	9.81e-20	1.000	437.5	9.71e-20	1.000	438.0	1.06e-19	1.000	438.5	1.16e-19	1.000
439.0	1.08e-19	1.000	439.5	1.05e-19	1.000	440.0	9.70e-20	1.000	440.5	1.01e-19	1.000	441.0	1.04e-19	1.000
441.5	1.07e-19	1.000	442.0	1.02e-19	1.000	442.5	9.68e-20	1.000	443.0	1.00e-19	1.000	443.5	1.14e-19	1.000
444.0	1.13e-19	1.000	444.5	1.03e-19	1.000	445.0	9.74e-20	1.000	445.5	8.46e-20	1.000	446.0	8.70e-20	1.000
446.5	9.97e-20	1.000	447.0	1.01e-19	1.000	447.5	9.15e-20	1.000	448.0	9.41e-20	1.000	448.5	8.99e-20	1.000
449.0	1.10e-19	1.000	449.5	9.12e-20	1.000	450.0	8.56e-20	1.000	450.5	8.28e-20	1.000	451.0	6.15e-20	1.000
451.5	5.56e-20	1.000	452.0	6.47e-20	1.000	452.5	7.27e-20	1.000	453.0	5.75e-20	1.000	453.5	5.08e-20	1.000
454.0	4.38e-20	1.000	454.5	3.81e-20	1.000	455.0	3.61e-20	1.000	455.5	3.61e-20	1.000	456.0	3.13e-20	1.000
456.5	2.72e-20	1.000	457.0	2.44e-20	1.000	457.5	2.22e-20	1.000	458.0	1.82e-20	1.000	458.5	1.43e-20	1.000
459.0	1.32e-20	1.000	459.5	1.05e-20	1.000	460.0	8.95e-21	1.000	460.5	8.90e-21	1.000	461.0	7.94e-21	1.000
461.5	7.04e-21	1.000	462.0	6.46e-21	1.000	462.5	5.63e-21	1.000	463.0	4.78e-21	1.000	463.5	3.94e-21	1.000
464.0	3.26e-21	1.000	464.5	2.97e-21	1.000	465.0	2.65e-21	1.000	465.5	2.46e-21	1.000	466.0	2.27e-21	1.000
466.5	2.08e-21	1.000	467.0	1.86e-21	1.000	467.5	1.76e-21	1.000	468.0	1.60e-21	1.000	468.5	1.44e-21	1.000
469.0	1.34e-21	1.000	469.5	1.20e-21	1.000	470.0	1.07e-21	1.000	470.5	1.02e-21	1.000	471.0	9.92e-22	1.000
471.5	9.97e-22	1.000	472.0	8.87e-22	1.000	472.5	8.27e-22	1.000	473.0	7.76e-22	1.000	473.5	7.15e-22	1.000
474.0	6.71e-22	1.000	474.5	6.67e-22	1.000	475.0	6.10e-22	1.000	475.5	6.17e-22	1.000	476.0	5.54e-22	1.000
476.5	5.22e-22	1.000	477.0	5.10e-22	1.000	477.5	5.17e-22	1.000	478.0	4.80e-22	1.000	478.5	4.71e-22	1.000
479.0	4.60e-22	1.000	479.5	4.35e-22	1.000	480.0	3.90e-22	1.000	480.5	3.71e-22	1.000	481.0	3.62e-22	1.000
481.5	3.52e-22	1.000	482.0	3.05e-22	1.000	482.5	3.05e-22	1.000	483.0	2.86e-22	1.000	483.5	2.53e-22	1.000
484.0	2.75e-22	1.000	484.5	2.59e-22	1.000	485.0	2.47e-22	1.000	485.5	2.36e-22	1.000	486.0	2.12e-22	1.000
486.5	1.89e-22	1.000	487.0	1.93e-22	1.000	487.5	1.86e-22	1.000	488.0	1.82e-22	1.000	488.5	1.75e-22	1.000
489.0	1.74e-22	1.000	489.5	1.72e-22	1.000	490.0	1.66e-22	1.000	490.5	1.75e-22	1.000	491.0	1.54e-22	1.000
491.5	1.74e-22	1.000	492.0	1.63e-22	1.000	492.5	1.53e-22	1.000	493.0	1.52e-22	1.000	493.5	5.85e-23	1.000
494.0	0.00e+00	1.000												

Table A-4. Chamber wall effect and background characterization parameters used in the environmental chamber model simulations for mechanism evaluation.

Cham.	Set [a]	Value	Discussion
<u>RN-I (ppb)</u>			
DTC	18	0.066	Ratio of the rate of wall + hv -> HONO to the NO ₂ photolysis rate. Average of value of RS-I that gave best fits to n-butane - NO _x chamber experiments carried out in this chamber. The initial HONO was optimized at the same time. If a temperature dependence is shown, it was derived from the temperature dependence of the RN-I values that best fit characterization data in outdoor chamber experiments, with the same activation energy used in all cases. If a temperature dependence is not shown, then the temperature variation for experiments in this set is small compared to the run-to-run variability in the best fit RN-I values. Note that the radical source in Sets 3, 12, 13, and 16 runs was anomalously high. Any dependence of apparent radical source on initial NO _x levels in Teflon bag chambers was found to be much less than the run-to-run variability.
<u>HONO-F (unitless)</u>			
DTC	18	0.8%	Ratio of the initial HONO concentration to the measured initial NO ₂ . [The initial NO ₂ in the experiment is reduced by a factor of 1 - (HONO-F)]. Unless the characterization data indicate otherwise, it is assumed that the initial HONO is introduced with the NO ₂ injection, so it is assumed to be proportional to the initial NO ₂ concentration. Average of value of initial HONO to initial NO ₂ that gave best fits to n-butane - NO _x chamber experiments carried out in this chamber. The RN-I parameter was optimized at the same time.
<u>E-NO₂/K1 (ppb)</u>			
All Teflon Bag Chambers		0	Ratio of rate of NO ₂ offgasing from the walls to the NO ₂ photolysis rate. The NO _x offgasing caused by representing the radical source by HONO offgasing appears to be sufficient for accounting for NO _x offgasing effects in most cases. RN-I parameters adjusted to fit experiments sensitive to the radical source are consistent with NO _x offgasing rates adjusted to fit pure air or aldehyde - air runs, to within the uncertainty and variability.
<u>k(NO₂W) (min⁻¹)</u>			
All Teflon Bag Chambers		1.6e-4	Rate of unimolecular loss (or hydrolysis) of NO ₂ to the walls. Based on dark NO ₂ decay and HONO formation measured in the ETC by Pitts et al. (1984). Assumed to be the same in all Teflon bag chambers, regardless of volume.
<u>YHONO</u>			
All Teflon Bag Chambers		0.2	Yield of HONO in the unimolecular reaction (hydrolysis) of NO ₂ on the walls. Based on dark NO ₂ decay and HONO formation measured in the ETC by Pitts et al. (1984). Assumed to be the same in all Teflon bag chambers, regardless of volume.
<u>k(O₃W) (min⁻¹)</u>			
DTC	All	1.5e-4	Unimolecular loss rate of O ₃ to the walls. Based on results of O ₃ decay in Teflon bag chambers experiments as discussed by Carter et al (1995c).
<u>k(N₂O₅) (min⁻¹)</u>			
All Teflon Bag Chambers		2.8e-3	Rate constant for N₂O₅ -> 2 Wall-NO_x . This represents the humidity-independent portion of the wall loss of N ₂ O ₅ , or the intercept of plots of rates of N ₂ O ₅ loss against humidity. Based on N ₂ O ₅ decay rate measurements made by Tuazon et al (1983) for the ETC. Assumed to be independent of chamber size (Carter et al, 1995c).

Table A-4 (continued)

Cham.	Set [a]	Value	Discussion
<u>k(N2O5) (ppm⁻¹ min⁻¹)</u>			
All Teflon Bag Chambers		1.1e-6	Rate constant for N2O5 + H2O -> 2 Wall-NOx . This represents the humidity dependent portion of the wall loss of N ₂ O ₅ , or the slope of plots of rates of N ₂ O ₅ loss against humidity. Based on N ₂ O ₅ decay rate measurements made by Tuazon et al (1983) for the ETC. Assumed to be independent of chamber size (Carter et al, 1995d).
<u>k(XSHC) (min⁻¹)</u>			
All Teflon Bag Chambers		250	Rate constant for OH -> HO2 . This represents the effects of reaction of OH with reactive VOCs in the background air or offgassed from the chamber walls. This parameter does not significantly affect model simulations of experiments other than pure air runs. Estimated from modeling several pure air in the ITC (Carter et al, 1996c), and also consistent with simulations of pure air runs in the ETC (Carter et al, 1997a).
<u>H2O (ppm)</u>			
DTC	all	1.0e+3	Default water vapor concentration for runs where no humidity data are available. Experiments in this chamber were carried out using dried purified air. The limited humidity data for such runs indicate that the humidity was less than 5%, probably no more than ~2.5%, and possibly much less than that. The default value corresponds to ~2.5 - 3% RH for the conditions of most experiments.

[a] Set refers to the characterization set, which refers to the group of experiments assumed to have the same run conditions and represented using the same chamber-dependent parameters. See Carter et al (1995) for more discussion. All experiments in this program were in DTC characterization set 18.